

Electronic Supporting Information

Free-Standing Blatter Radical Polymer Thin Films: Precise Nanometer Thickness Tuning and Redox-Optical Properties

*Monika Yadav,^a Saurabh Kumar Rajput,^a Anjali Prodhuku,^b Manas Kumar Pati,^a Mahesh Kumar Ravva,^b Victor Chechik^c and Venkata Suresh Mothika^{*a}*

^aDepartment of Chemistry, Indian Institute of Technology (IIT) Kanpur, Kanpur, 208016, India

^bDepartment of Chemistry, Centre for Computational and Integrative Sciences, SRM University-AP, Amravati, India 522240

^cDepartment of Chemistry, University of York, York YO10 5DD, United Kingdom

**E-mail: smothika@iitk.ac.in*

List of Contents

1a. Materials and methods.	S3
1b Instrumentation.	S4
2. Synthesis routes.	S6
3. Crystallographic data and parameters.	S9
4. DFT-optimized geometries of Cz_3N^{\bullet} and Cz_2N^{\bullet} using DCM as solvent.	S15
5. Electrochemical studies of monomers Cz_3N^{\bullet} and Cz_2N^{\bullet} .	S19
6. Electropolymerization studies of Cz_3N^{\bullet} and Cz_2N^{\bullet} .	S20
7. AFM of polymeric thin film of poly Cz_3N^{\bullet} and poly Cz_2N^{\bullet} .	S21
8. FTIR spectra of Cz_3N^{\bullet} , Cz_2N^{\bullet} , poly Cz_3N^{\bullet} and poly Cz_2N^{\bullet} .	S25
9. Thermogravimetric analysis (TGA) of Cz_3N^{\bullet} , Cz_2N^{\bullet} , poly Cz_3N^{\bullet} and poly Cz_2N^{\bullet} .	S26
10. Air-stability of monomer Cz_3N^{\bullet} radical examined by solution state UV-Vis absorption spectroscopy.	S27
11. XPS studies of monomers and polymer Blatter radicals	S27
12. Concentration-dependent absorption spectra of radical monomers.	S28
13. Band gap calculation for monomer radicals, Cz_3N^{\bullet} , Cz_2N^{\bullet} and oxidised species Cz_3N^{+} , Cz_2N^{+} and for polymeric thin film poly Cz_3N^{\bullet} and poly Cz_2N^{\bullet} .	S29
14. DFT-optimized geometries of Cz_3N^{+} and Cz_2N^{+} using DCM as solvent.	S30
15. Experimentally calculated HOMO-LUMO and band gap for Cz_3N^{\bullet} , Cz_2N^{\bullet} , poly Cz_3N^{\bullet} , and poly Cz_2N^{\bullet} .	S34
16. EPR studies of Cz_3N^{\bullet} and Cz_2N^{\bullet} .	S35
17. References	S36

1a. Materials and methods.

4-Bromo-2-fluoro-1-nitrobenzene, (4-(9H-carbazol-9-yl)phenyl)boronic acid and 4-Bromophenyl hydrazine were purchased from BLD Pharma. Tetrakis(triphenylphosphine)palladium (0) and potassium carbonate were purchased from Merck. Cesium carbonate was purchased from SRL. Phenyl hydrazine, acetic acid, and sodium hydroxide were purchased from CDH, Finar and Qualigens, respectively. 4-Bromobenzoyl chloride and tin (powder) were purchased from Spectrochem and Sigma Aldrich, respectively. Freshly distilled tetrahydrofuran, dichloromethane, acetonitrile, and triethylamine were used for the synthesis of radical derivatives. Hexane, acetone, and isopropyl alcohol were purchased from Finar chemicals and used as received for the cleaning of ITO substrates. Indium-tin oxide-coated glass substrates (ITO, thickness: 1.1 mm, sheet resistance: $<10 \Omega\text{sq}^{-1}$) were purchased from Nanoshel.

Geometry optimizations of cationic and radical geometries of compounds 1 and 2 were carried out using the B3LYP/6-31G** level of theory. Implicit solvent effects were included using the polarizable continuum model (PCM) and dichloromethane is used as the solvent. Single-point energy calculations were then carried out at the B3LYP/6-31+G** level of theory using the optimized geometries. All calculations were performed using the Gaussian 16 software package.¹

Magnetic measurements were carried out by initially cooling the radicals (Zero Field Cooling), followed by application of an external magnetic field upon heating in the temperature range 4 – 300 K at a rate of 2 K/min using the Physical Property Measurement System (PPMS).

Analysis for $\text{Cz}_3\text{N}^\bullet$

$\text{Cz}_3\text{N}^\bullet$ ($m = 7 \text{ mg}$, $M_w = 1008 \text{ g mol}^{-1}$) was analysed upon heating in the range 4 – 300 K at 0.1 T.

Analysis of Cz₃N• dimers.

The magnetic susceptibility data were further analysed considering a radical dimer of spins ($S = \frac{1}{2}$) for Cz₃N• ($m = 7$ mg, $M_w = 2016$ g mol⁻¹) at 0.1 T in the temperature range of 4 – 300 K.

All the fitting equations were adopted from the literature.¹⁰

1b. Instrumentation.

¹H NMR spectra for compounds were recorded on ECX 400 MHz JOEL model spectrometers, where all spectra were taken in deuterated chloroform from Sigma Aldrich, and TMS was used as an external standard. Absorption spectra of radicals were collected on JASCO V-670 and used for calculating the molar extinction coefficient. Mass spectra were recorded on LC-MS (ESI)-QToF (Agilent 6546). EPR spectra were recorded at X band (9.1 GHz) on a JEOL X320 spectrometer. Typical acquisition parameters: modulation frequency 100 kHz, modulation amplitude 0.1 mT, microwave power 1 mW. The spectra were recorded at 323 K with 1 mM solutions of Blatter's radicals in degassed toluene. EPR spectra were simulated using EasySpin software.² Fourier transform infrared spectroscopy (FTIR) measurements were performed in ATR mode using a Perkin Elmer 1000 UATR instrument in the range of 400 – 4000 cm⁻¹. The thermal stability of radicals was assessed using a TGA/DSC 1 Star instrument from Mettler Toledo under an inert atmosphere in the temperature range of 25 to 1000 °C at a heating rate of 10 °C/min. The electrochemical measurements were performed on the PalmSens PS4.F2.05 workstation. Electrochemical studies were carried out in a three-electrode electrochemical cell containing a glassy carbon electrode, GC (working electrode), Ag/AgCl electrode in 0.1 M KCl (reference electrode), and a platinum wire (counter electrode).

Single-crystal X-ray studies were conducted on a CCD Bruker SMART APEX diffractometer equipped with an Oxford Instruments low-temperature attachment. Data were collected at

100(2) K using graphite monochromatic Mo K α radiation ($\lambda = 0.71073$ Å). The frames were indexed, integrated, and scaled using the SMART and SAINT software packages,³ and the data were corrected for absorption using the SADABS program.⁴ The structures were solved and refined with the SHELXL⁵ and OLEX2⁶ suites of programs, while additional crystallographic calculations were performed by the program PLATON. All hydrogen atoms were included in the final stages of the refinement and were refined with a typical “riding model”. Disordered solvent molecules in the unit cell have been masked using the Olex-2 mask program. The crystallographic figures have been generated using Olex2 software. CCDC number 2502298 contain supplementary crystallographic data for Cz₃N*, respectively. These data can be obtained free of charge from the Cambridge Crystallographic Data Centre via www.ccdc.cam.ac.uk/data_request/cif. MestRe Nova software for NMR analysis and OriginPro22 software for plotting curves were used.

The thickness measurements of film were done by Bruker Optical profilometer instrument. The data collected with dual-LED illuminated optical module 2.5X and capable stitching with motorized XY stage. The commercial Asylum Research (Oxford Instruments) was used to conduct the AFM analysis, and a silicon probe with a force constant of 0.5 N m⁻¹ was used. A Thermo Scientific NEXSA Surface Analysis instrument, having a monochromatic Al K α line source ($h\nu = 1486.69$ eV), was used for X-ray photoelectron spectroscopy (XPS) measurements.

Fitting procedure for XPS fitting:

The XPS fitting was carried out according to the available tutorials. Initially, background subtraction was performed using Shirley's method. Then the XPS peaks are fitted using Gaussian functions, with full width at half maximum (FWHM) less than 2 eV for each peak. Peak identification was carried out on the basis of known binding energy values obtained from

existing literature, allowing the assignment of peaks for elements of different chemical environments.

2. Synthesis routes

Synthesis of compound **1** and **2** according to the literature.^{7,8}

Synthesis of 4-bromo-N'-(5-bromo-2-nitrophenyl)-N'-phenylbenzohydrazide (3): A sealed tube was charged with **1** (300 mg, 1.03 mmol), 4-bromo-2-fluoro-nitrobenzene (340 mg, 1.545 mmol), potassium carbonate (156 mg, 1.133 mmol), ethyl alcohol (10 mL), and the reaction mixture was stirred at 110 °C for 48 h. The reaction mixture was then cooled to room temperature and extracted with CH₂Cl₂. The organic layer was collected, concentrated under reduced pressure, and crude solids were purified using column chromatography to get compound **3**. Yield: 40 %. ¹H NMR (400 MHz, CDCl₃) δ 8.54 (s, 1H), 7.95 (d, *J* = 2.2 Hz, 1H), 7.89 (d, *J* = 8.7 Hz, 1H), 7.68 (d, *J* = 8.7 Hz, 2H), 7.62 (d, *J* = 8.6 Hz, 2H), 7.48 (dd, *J* = 8.8, 2.1 Hz, 1H), 7.29 (dd, *J* = 8.7, 7.4 Hz, 2H), 7.04 (t, *J* = 7.5 Hz, 1H), 6.96 – 6.91 (m, 2H). Calculated: 488.9324 found [M+H]⁺ *m/z*: 489.9398.

Synthesis of 4-bromo-N'-(5-bromo-2-nitrophenyl)-N'-(4-bromophenyl)benzohydrazide (4): A sealed tube was charged with **2** (300 mg, 0.81 mmol), 4-bromo-2-fluoro-nitrobenzene (267 mg, 1.216 mmol), potassium carbonate (123 mg, 0.891 mmol), ethyl alcohol (10 mL), and the reaction mixture was stirred at 110 °C for 48 h. The reaction mixture was then cooled to room temperature and extracted with CH₂Cl₂. The organic layer was collected, concentrated under reduced pressure, and crude solids were purified using column chromatography to get compound **4**. Yield: 35 %. ¹H NMR (400 MHz, CDCl₃) δ 8.59 (s, 1H), 7.95 (d, *J* = 1.9 Hz, 1H), 7.67 – 7.60 (m, 4H), 7.52 (d, *J* = 8.3 Hz, 2H), 7.36 (d, *J* = 8.6 Hz, 3H), 6.76 (d, *J* = 9.0 Hz, 1H). Calculated: 566.8429 found [M+Na]⁺ *m/z*: 589.8314.

Synthesis of Br₂N[•]: Blatter radical Br₂N[•] was synthesized by adopting the literature procedures.⁹ In a 100 mL round-bottom flask, compound **3** (500 mg, 1.02 mmol) was dissolved in acetic acid (10 mL), followed by the addition of tin powder (602 mg, 5.1 mmol) over 30 min under vigorous stirring and then heated at 118 °C for 10 min. The reaction mixture was then cooled to room temperature and diluted with CH₂Cl₂, followed by neutralisation with 2M NaOH. The obtained products were dissolved in CH₂Cl₂ (50 mL) and added with 2M NaOH (50 mL) and allowed to stir for 12 h at room temperature. The organic layer was separated and washed three times with distilled water. The organic fractions were concentrated under reduced pressure, and the crude was purified by column chromatography using basic aluminium oxide (CH₂Cl₂:hexane, 50:50) to get Br₂N[•] as dark green needles. Yield: 85%. Calculated: 439.9398 found [M]⁺ m/z: 439.9397. ν_{\max} / cm⁻¹ 3063w (aryl C–H), 1591w, 1474s, 1430w, 1391s, 1307w, 1267w, 1238w, 1190m, 1171w, 1102w, 1070w, 1009w, 961w, 888m, 851m, 822w, 801w, 755w, 718m, 687s, 670w.

Synthesis of Br₃N[•]: Following a similar procedure to that for the synthesis of Br₂N[•]. In a 100 ml round-bottom flask, compound **4** (500 mg, 0.883 mmol) was dissolved in acetic acid (10 ml), followed by the addition of tin powder (521 mg, 4.416 mmol) over 30 min under vigorous stirring and then heated at 118 °C for 10 min. The reaction mixture was then cooled to room temperature and diluted with CH₂Cl₂, followed by neutralisation with 2M NaOH. The obtained products were dissolved in CH₂Cl₂ (50 mL) and added with 2M NaOH (50 mL), and allowed to stir for 12 h at room temperature. The organic layer was separated and washed three times with distilled water. The organic fractions were concentrated under reduced pressure, and the crude was purified by column chromatography using basic aluminium oxide (CH₂Cl₂:hexane, 50:50) to get Br₃N[•] as dark green needles. Yield: 60%. Calculated: 517.8503 found [M]⁺ m/z: 517.8504. ν_{\max} / cm⁻¹ 3070w (aryl C–H), 1590w, 1566w, 1475s, 1417m, 1392s, 1338w, 1306w,

1263w, 1242w, 1188w, 1172w, 1103w, 1066s, 1007s, 948w, 887m, 836m, 815s, 740w, 719m, 702w, 669m.

Synthesis of Cz₂N[•]: A 100 mL Schlenk flask loaded with radical **Br₂N[•]** (75 mg, 0.169 mmol), (4-(9H-carbazol-9-yl)phenyl)boronic acid (146 mg, 0.509 mmol), Pd(PPh₃)₄ (10 mg, 5 mol%), Cs₂CO₃ (5mg, 10 mol%) and all reagents were subjected to vacuum and nitrogen gas purging three cycles to ensure inert atmosphere. To this THF: H₂O (5:1) 20 mL was added, and the mixture was heated at 70 °C for 12 h. The reaction mixture was cooled to room temperature and then extracted with CH₂Cl₂. The organic fractions were collected and concentrated under reduced pressure. The crude solids were then purified by column chromatography using basic aluminium oxide (CH₂Cl₂:hexane) to get dark reddish-brown compound Cz₂N[•]. Yield: 60%. Calculated: 766.2971 found [M]⁺ m/z: 766.2972. ν_{\max} / cm⁻¹ 3043w (aryl C–H), 1603w, 1594w, 1526w, 1499m, 1449m, 1389w, 1360w, 1333w, 1318w, 1223w, 1175w, 1016w, 1004w, 913w, 900w, 842m, 830m, 817m, 770w, 749s, 720s, 693m, 683m, 646w.

Synthesis of Cz₃N[•]: A 100 mL Schlenk flask loaded with radical **Br₃N[•]** (75 mg, 0.145 mmol), (4-(9H-carbazol-9-yl)phenyl)boronic acid (187 mg, 0.652 mmol), Pd(PPh₃)₄ (17 mg, 10 mol%), Cs₂CO₃ (14mg, 30 mol%) and all reagents were subjected to vacuum and nitrogen gas purging three cycles to ensure inert atmosphere. To this THF: H₂O (5:1) 20 mL was added, and the mixture was heated at 70 °C for 12 h. The reaction mixture was cooled to room temperature and then extracted with CH₂Cl₂. The organic fractions were collected and concentrated under reduced pressure. The crude solids were then purified by column chromatography using basic aluminium oxide (CH₂Cl₂:hexane) to get dark reddish-brown compound Cz₃N[•]. Yield: 65%. Calculated: 1007.3862 found [M]⁺ m/z: 1007.3861. ν_{\max} / cm⁻¹ 3048w (aryl C–H), 1623w, 1597w, 1493m, 1479m, 1450m, 1398w, 1362w, 1334w, 1315w, 1227m, 1170w, 1004w, 915w, 900w, 823w, 746s, 724s, 685w, 637w, 623w.

3. Crystallographic data and parameters.

Table S1. Crystallographic data and structural refinement for $\text{Cz}_3\text{N}^{\bullet}$.

	$\text{Cz}_3\text{N}^{\bullet}$
Empirical formula	$\text{C}_{73}\text{H}_{47}\text{N}_6$
Formula Weight	1008.227 g mol ⁻¹
Crystal System	Monoclinic
Space Group	$P2_1/c$
Temperature (K)	296.15
a (Å)	19.8107(10)
b (Å)	14.1961(8)
c (Å)	20.7394(11)
α (°)	90
β (°)	103.349(2)
γ (°)	90
V (Å ³)	5675.1(5)
Z	4
ρ_{calcd} (g cm ⁻³)	1.180
μ (mm ⁻¹)	0.069
F (000)	2109.2
Crystal size (mm ³)	0.20 × 0.19 × 0.18
Radiation	Mo K α ($\lambda = 0.71073$ Å)
Index ranges	-26 ≤ h ≤ 26, -18 ≤ k ≤ 18, -27 ≤ l ≤ 27
Reflections collected	117394
Independent reflections	14147
2 θ range for data collection (°)	4.32 to 56.72
Data/restraints/parameters	14147/0/712
Goof	1.059
R _{int}	0.1006
Final R indices [I > 2 σ (I)]	R ₁ = 0.1143, wR ₂ = 0.2588

R indices (all data)	$R_1 = 0.1451$, $wR_2 = 0.2783$
Largest diff. peak/hole / $e \text{ \AA}^{-3}$	0.72/-0.61
CCDC number	2502298

Table S2. Bond lengths obtained from the single crystal structure of $\text{Cz}_3\text{N}^{\bullet}$.

$\text{Cz}_3\text{N}^{\bullet}$			
Atom-Atom	Bond Length / \AA	Atom-Atom	Bond Length / \AA
N001 N002	1.364(3)	C00U C011	1.384(4)
N001 C00B	1.382(4)	C00W C010	1.391(5)
N001 C00S	1.441(4)	C00W C016	1.398(5)
N002 C00F	1.341(4)	C00X C01A	1.414(4)
N003 C00F	1.330(4)	C00Y C00Z	1.378(5)
N003 C00I	1.376(4)	C00Z C019	1.390(5)
N004 C00A	1.424(4)	C010 C01G	1.415(4)
N004 C010	1.399(4)	C013 C01S	1.366(5)
N004 C01E	1.393(4)	C013 C01T	1.399(5)
N005 C00X	1.395(4)	C014 C019	1.387(4)
N005 C00Z	1.422(4)	C015 C01D	1.383(5)
N005 C01V	1.405(4)	C016 C018	1.386(5)
C006 C00D	1.396(4)	C017 C01B	1.394(4)
C006 C00N	1.478(4)	C018 C01Q	1.374(6)
C006 C00T	1.399(4)	C01A C01D	1.388(5)
C007 C00B	1.387(4)	C01A C01R	1.435(5)
C007 C00N	1.393(4)	C01C C01K	1.359(6)
N008 C01F	1.421(4)	C01C C01N	1.410(5)
N008 C01H	1.406(5)	C01E C01J	1.410(5)
N008 C01O	1.390(5)	C01E C01W	1.386(5)
C009 C00A	1.390(4)	C01F C01P	1.359(6)
C009 C00D	1.382(4)	C01F C01U	1.396(5)
C00A C00K	1.387(4)	C01G C01J	1.418(5)
C00B C00I	1.415(4)	C01G C01Q	1.400(5)

C00C C00P	1.393(4)	C01H C01M	1.374(6)
C00C C00U	1.494(4)	C01H C01N	1.403(5)
C00C C014	1.400(4)	C01I C01N	1.424(6)
C00E C00F	1.490(4)	C01I C01O	1.411(5)
C00E C00G	1.393(4)	C01I C01X	1.399(6)
C00E C00O	1.389(4)	C01J C021	1.415(5)
C00G C00R	1.384(4)	C01K C01L	1.362(6)
C00H C00J	1.386(5)	C01L C01M	1.395(5)
C00H C012	1.387(4)	C01O C01Z	1.368(6)
C00I C00V	1.398(4)	C01P C01S	1.410(5)
C00J C013	1.492(4)	C01R C01V	1.401(5)
C00J C017	1.399(5)	C01R C022	1.409(5)
C00K C00T	1.378(4)	C01T C01U	1.386(5)
C00L C00M	1.384(5)	C01V C01Y	1.395(6)
C00L C00X	1.387(5)	C01W C025	1.385(5)
C00M C015	1.389(5)	C01X C020	1.359(7)
C00N C00Q	1.415(4)	C01Y C026	1.377(5)
C00O C011	1.388(4)	C01Z C023	1.380(6)
C00P C00Y	1.382(4)	C020 C023	1.392(6)
C00Q C00V	1.373(4)	C021 C027	1.371(7)
C00R C00U	1.397(4)	C022 C024	1.373(7)
C00S C012	1.380(5)	C024 C026	1.396(7)
C00S C01B	1.374(5)	C025 C027	1.392(7)

Table S3. Selected bond angles of obtained from the single crystal structure of Cz_3N^+ .

Cz_3N^+			
Atom-Atom -Atom	Bond Angle / °	Atom-Atom -Atom	Bond Angle / °
N002 N001 C00B	122.9(2)	C00W C010 N004	129.4(3)
N002 N001 C00S	115.2(2)	C00W C010 C01G	121.9(3)
C00B N001 C00S	121.2(2)	C00U C011 C00O	121.0(3)
C00F N002 N001	115.0(2)	C00S C012 C00H	119.1(3)
C00F N003 C00I	115.2(2)	C01S C013 C00J	120.5(3)

C010	N004	C00A	125.1(3)	C01S	C013	C01T	119.0(3)
C01E	N004	C00A	125.7(3)	C01T	C013	C00J	120.5(3)
C01E	N004	C010	108.4(3)	C019	C014	C00C	121.8(3)
C00X	N005	C00Z	124.9(3)	C01D	C015	C00M	120.7(3)
C00X	N005	C01V	108.1(3)	C018	C016	C00W	121.8(3)
C01V	N005	C00Z	125.5(3)	C01B	C017	C00J	120.4(3)
C00D	C006	C00N	120.7(3)	C01Q	C018	C016	120.8(3)
C00D	C006	C00T	117.5(3)	C014	C019	C00Z	119.6(3)
C00T	C006	C00N	121.7(3)	C00X	C01A	C01R	107.0(3)
C00B	C007	C00N	120.3(3)	C01D	C01A	C00X	119.4(3)
C01H	N008	C01F	126.4(3)	C01D	C01A	C01R	133.5(3)
C01O	N008	C01F	125.4(3)	C00S	C01B	C017	118.7(3)
C01O	N008	C01H	108.0(3)	C01K	C01C	C01N	120.4(4)
C00D	C009	C00A	119.9(3)	C015	C01D	C01A	119.0(3)
C009	C00A	N004	120.0(3)	N004	C01E	C01J	108.0(3)
C00K	C00A	N004	120.4(3)	C01W	C01E	N004	129.0(3)
C00K	C00A	C009	119.5(3)	C01W	C01E	C01J	122.8(3)
N001	C00B	C007	122.3(3)	C01P	C01F	N008	120.8(3)
N001	C00B	C00I	116.4(3)	C01P	C01F	C01U	119.8(3)
C007	C00B	C00I	121.3(3)	C01U	C01F	N008	119.4(4)
C00P	C00C	C00U	120.8(3)	C010	C01G	C01J	106.5(3)
C00P	C00C	C014	116.8(3)	C01Q	C01G	C010	118.8(3)
C014	C00C	C00U	122.3(3)	C01Q	C01G	C01J	134.7(3)
C009	C00D	C006	121.5(3)	C01M	C01H	N008	129.8(3)
C00G	C00E	C00F	120.0(3)	C01M	C01H	C01N	121.4(3)
C00O	C00E	C00F	121.9(3)	C01N	C01H	N008	108.8(4)
C00O	C00E	C00G	118.1(3)	C01O	C01I	C01N	107.6(3)
N002	C00F	C00E	114.1(2)	C01X	C01I	C01N	134.0(3)
N003	C00F	N002	128.5(3)	C01X	C01I	C01O	118.3(4)
N003	C00F	C00E	117.3(2)	C01E	C01J	C01G	108.3(3)
C00R	C00G	C00E	121.1(3)	C01E	C01J	C021	118.7(4)
C00J	C00H	C012	120.6(3)	C021	C01J	C01G	132.9(4)
N003	C00I	C00B	121.7(3)	C01C	C01K	C01L	119.7(4)

N003 C00I C00V	120.2(3)	C01K C01L C01M	122.7(4)
C00V C00I C00B	118.0(3)	C01H C01M C01L	117.4(4)
C00H C00J C013	121.3(3)	C01C C01N C01I	134.6(3)
C00H C00J C017	119.2(3)	C01H C01N C01C	118.3(4)
C017 C00J C013	119.4(3)	C01H C01N C01I	107.0(3)
C00T C00K C00A	120.2(3)	N008 C01O C01I	108.5(3)
C00M C00L C00X	117.3(3)	C01Z C01O N008	129.2(3)
C00L C00M C015	121.8(3)	C01Z C01O C01I	122.3(4)
C007 C00N C006	120.5(3)	C01F C01P C01S	120.2(4)
C007 C00N C00Q	118.3(3)	C018 C01Q C01G	119.6(3)
C00Q C00N C006	121.3(3)	C01V C01R C01A	107.3(3)
C011 C00O C00E	120.9(3)	C01V C01R C022	119.4(4)
C00Y C00P C00C	122.0(3)	C022 C01R C01A	133.2(4)
C00V C00Q C00N	121.5(3)	C013 C01S C01P	120.6(4)
C00G C00R C00U	120.6(3)	C01U C01T C013	120.5(4)
C012 C00S N001	118.8(3)	C01T C01U C01F	119.8(4)
C01B C00S N001	119.2(3)	C01R C01V N005	108.8(3)
C01B C00S C012	122.0(3)	C01Y C01V N005	129.2(3)
C00K C00T C006	121.4(3)	C01Y C01V C01R	122.0(3)
C00R C00U C00C	120.4(3)	C025 C01W C01E	116.6(4)
C011 C00U C00C	121.3(3)	C020 C01X C01I	119.5(4)
C011 C00U C00R	118.4(3)	C026 C01Y C01V	117.3(4)
C00Q C00V C00I	120.6(3)	C01O C01Z C023	117.6(4)
C010 C00W C016	117.0(3)	C01X C020 C023	120.9(4)
N005 C00X C01A	108.7(3)	C027 C021 C01J	118.5(4)
C00L C00X N005	129.6(3)	C024 C022 C01R	118.5(4)
C00L C00X C01A	121.7(3)	C01Z C023 C020	121.4(5)
C00Z C00Y C00P	120.0(3)	C022 C024 C026	121.2(4)
C00Y C00Z N005	119.5(3)	C01W C025 C027	122.1(4)
C00Y C00Z C019	119.7(3)	C01Y C026 C024	121.8(4)
C019 C00Z N005	120.7(3)	C021 C027 C025	121.3(4)
N004 C010 C01G	108.7(3)		

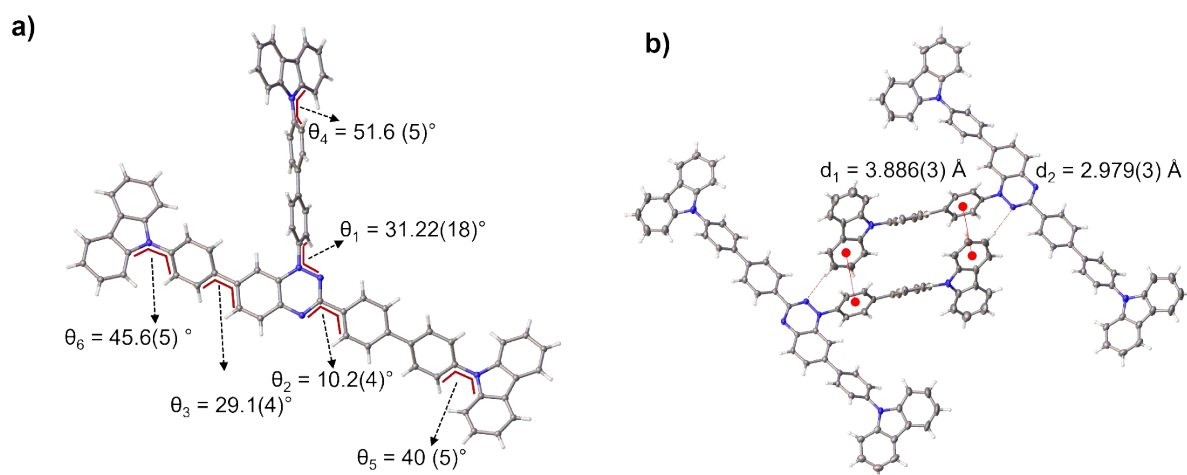


Fig. S1 Solid-state structure of Cz_3N^+ : a) representing different dihedral angles by (θ_1 to θ_6), b) representing key additional $\pi \cdots \pi$ interactions ($d_1 = 3.886(3) \text{ \AA}$), and $CH \cdots N$ contacts ($d_2 = 2.979(3) \text{ \AA}$) present.

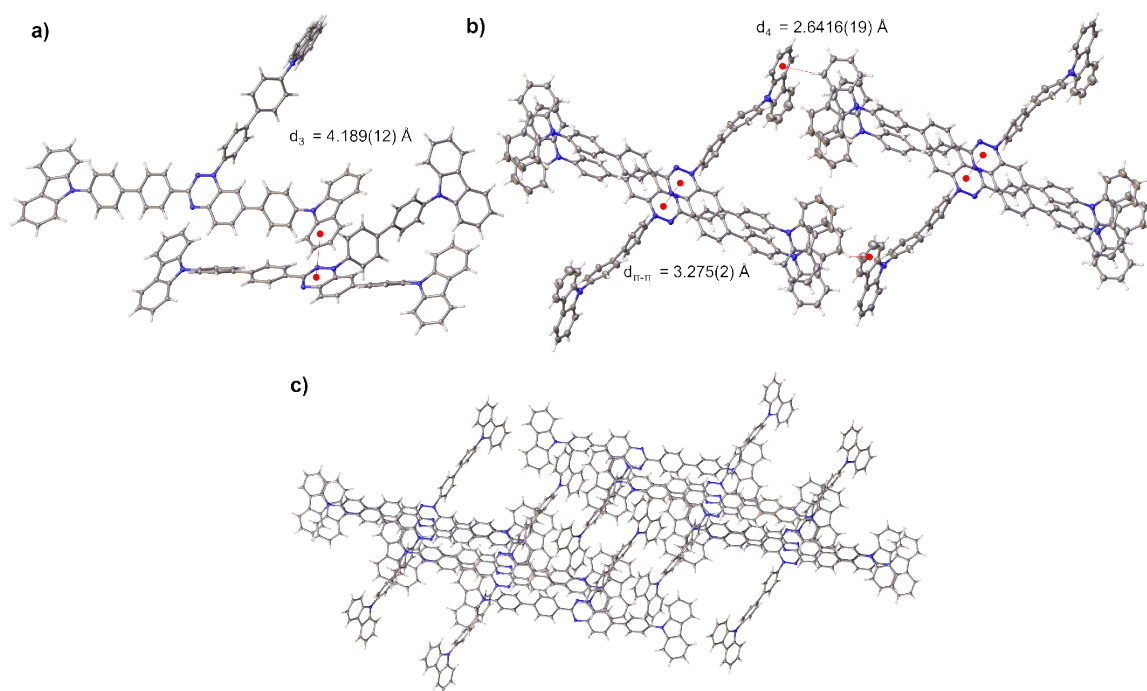
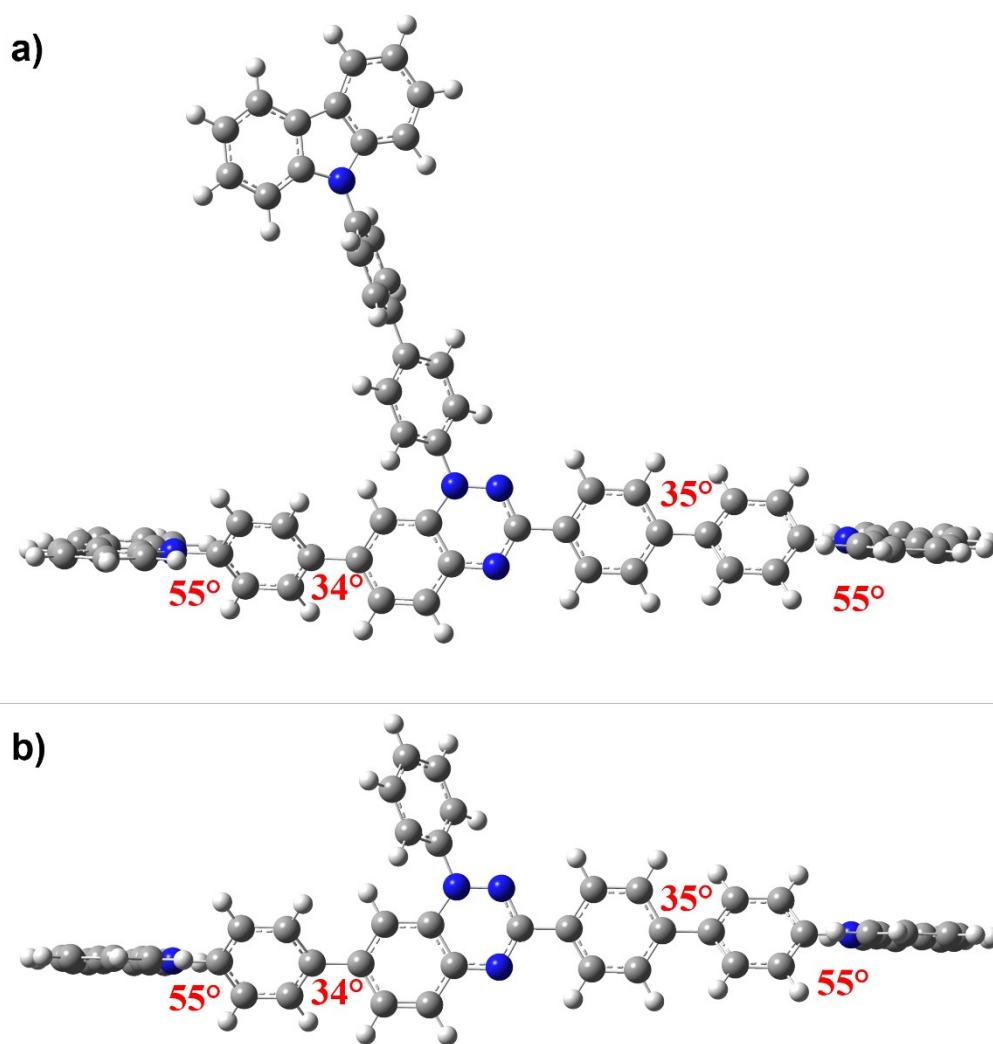


Fig. S2 Solid-state structure analysis of Cz_3N^+ : a) representing additional $\pi \cdots \pi$ interactions ($d_3 = 4.189(12) \text{ \AA}$), b) $CH \cdots \pi$ interactions ($d_4 = 2.6416(19) \text{ \AA}$) and c) solid-state packing along the b -direction.



4. DFT-optimized geometries of Cz_3N^+ and Cz_2N^+ using DCM as solvent.

Fig. S3 DFT-optimized geometries of a) Cz_3N^+ and b) Cz_2N^+ . The corresponding torsional angles were shown at each twisted center.

Table S4. Cartesian coordinates.

Cz ₃ N*				Cz ₂ N*			
6	1.297691000	-5.212643000	-0.503173000	6	3.614122000	-1.341704000	-1.700434000
6	-0.053755000	-4.933203000	-0.599734000	6	2.233742000	-1.327625000	-1.795489000
6	-0.532352000	-3.610549000	-0.508310000	6	1.457354000	-0.467233000	-0.993449000
6	0.422960000	-2.564709000	-0.349500000	6	2.140254000	0.413538000	-0.105030000
6	1.784460000	-2.858837000	-0.215436000	6	3.534079000	0.369546000	0.009807000
6	2.241500000	-4.181341000	-0.295977000	6	4.289786000	-0.501816000	-0.786571000
1	1.638206000	-6.237887000	-0.601928000	1	4.185778000	-1.997383000	-2.348623000
1	-0.782861000	-5.723504000	-0.743489000	1	1.710932000	-1.980581000	-2.486287000
1	2.487942000	-2.061024000	-0.016470000	1	4.030530000	0.992955000	0.741856000
6	-2.247856000	-2.091710000	-0.356294000	6	-0.566548000	0.276866000	-0.202335000
6	3.685596000	-4.488215000	-0.165125000	6	5.766741000	-0.539654000	-0.667961000
6	4.665405000	-3.606534000	-0.655679000	6	6.505310000	0.622555000	-0.381597000
6	4.121487000	-5.672953000	0.455179000	6	6.476855000	-1.742044000	-0.836485000
6	6.022008000	-3.887353000	-0.523824000	6	7.890854000	0.586504000	-0.256871000
1	4.364831000	-2.693143000	-1.158589000	1	5.992552000	1.571849000	-0.265276000
6	5.475701000	-5.970927000	0.572968000	6	7.864071000	-1.782850000	-0.733767000
1	3.393782000	-6.367294000	0.862395000	1	5.938354000	-2.662062000	-1.038995000
6	6.437893000	-5.076356000	0.088000000	6	8.582399000	-0.617773000	-0.437353000
1	6.762193000	-3.186448000	-0.894768000	1	8.440213000	1.491258000	-0.019507000
1	5.790981000	-6.897499000	1.040717000	1	8.393976000	-2.717537000	-0.882999000
6	-3.704021000	-1.795665000	-0.296436000	6	-2.051293000	0.194329000	-0.185512000
6	-4.637230000	-2.838999000	-0.390870000	6	-2.713232000	-0.725612000	-1.012538000
6	-4.180861000	-0.483951000	-0.143462000	6	-2.822728000	1.019953000	0.647840000
6	-6.002339000	-2.579141000	-0.333871000	6	-4.101034000	-0.817096000	-1.005848000
1	-4.276478000	-3.854831000	-0.500262000	1	-2.124000000	-1.372377000	-1.651800000
6	-5.546100000	-0.227713000	-0.086255000	6	-4.209784000	0.925671000	0.652381000
1	-3.473037000	0.334149000	-0.080719000	1	-2.326549000	1.743428000	1.283893000
6	-6.487859000	-1.268584000	-0.179851000	6	-4.880574000	0.005449000	-0.173573000
1	-6.701027000	-3.408551000	-0.383686000	1	-4.585455000	-1.555835000	-1.636837000
1	-5.887592000	0.798605000	0.006196000	1	-4.782849000	1.594370000	1.287137000
7	-0.099795000	-1.269495000	-0.293890000	7	1.328317000	1.264566000	0.648529000
7	-1.441331000	-1.033252000	-0.227420000	7	-0.030703000	1.155474000	0.651494000
7	-1.877453000	-3.365884000	-0.544376000	7	0.091887000	-0.511837000	-1.062917000
6	0.703783000	-0.088542000	-0.243079000	6	1.836828000	2.277629000	1.523851000
6	0.430071000	0.885789000	0.722704000	6	1.382871000	2.324953000	2.846002000
6	1.720243000	0.126265000	-1.180595000	6	2.737562000	3.236531000	1.046925000
6	1.181016000	2.055384000	0.757537000	6	1.845974000	3.328370000	3.695281000
1	-0.374974000	0.723511000	1.429697000	1	0.674571000	1.581099000	3.192090000
6	2.470205000	1.297563000	-1.130741000	6	3.199167000	4.232101000	1.907975000
1	1.917610000	-0.611582000	-1.950239000	1	3.058381000	3.213015000	0.011183000
6	2.219863000	2.285426000	-0.162474000	6	2.757398000	4.280587000	3.231889000
1	0.943522000	2.809939000	1.500267000	1	1.496794000	3.362296000	4.722536000
1	3.268493000	1.439279000	-1.851752000	1	3.894538000	4.978179000	1.536479000
6	-7.944336000	-0.992314000	-0.118271000	1	3.117198000	5.058972000	3.897299000
6	-8.857746000	-1.737372000	-0.884585000	6	-6.360951000	-0.093642000	-0.166283000
6	-8.456634000	0.022934000	0.708484000	6	-7.076150000	-0.368552000	-1.345097000
6	-10.225878000	-1.488434000	-0.822233000	6	-7.094698000	0.083835000	1.019812000
1	-8.494132000	-2.516081000	-1.547166000	6	-8.464247000	-0.472838000	-1.340795000
6	-9.821338000	0.291895000	0.761990000	1	-6.541909000	-0.492694000	-2.281514000
1	-7.781023000	0.604770000	1.327085000	6	-8.484184000	0.000766000	1.029550000

6	-10.717615000	-0.466759000	-0.000699000	1	-6.572588000	0.279291000	1.950895000
1	-10.916200000	-2.084777000	-1.409324000	6	-9.179525000	-0.283791000	-0.152013000
1	-10.195652000	1.090170000	1.394058000	1	-8.996995000	-0.701291000	-2.257787000
6	8.748403000	-5.422791000	-0.833393000	1	-9.033523000	0.156242000	1.952009000
6	8.491403000	-5.663836000	1.409177000	6	10.901873000	0.135456000	-1.038197000
6	8.548952000	-5.237067000	-2.205001000	6	10.726949000	-1.494567000	0.532029000
6	10.024582000	-5.750726000	-0.306461000	6	10.653580000	1.093456000	-2.026230000
6	7.998457000	-5.701958000	2.717267000	6	12.223396000	-0.197515000	-0.642582000
6	9.861083000	-5.902148000	1.124645000	6	10.267470000	-2.433074000	1.461358000
6	9.654216000	-5.366278000	-3.043973000	6	12.111705000	-1.235896000	0.360864000
1	7.569064000	-5.003805000	-2.606184000	6	11.751326000	1.730400000	-2.601945000
6	11.119002000	-5.874071000	-1.171817000	1	9.643336000	1.333035000	-2.338519000
6	8.896581000	-6.002018000	3.739737000	6	13.309024000	0.458193000	-1.236892000
1	6.954738000	-5.502853000	2.933007000	6	11.219121000	-3.126058000	2.207193000
6	10.742553000	-6.202030000	2.171012000	1	9.208097000	-2.616020000	1.601864000
6	10.928512000	-5.677594000	-2.536946000	6	13.047372000	-1.946936000	1.122952000
1	9.524485000	-5.224895000	-4.112850000	6	13.066877000	1.422076000	-2.211975000
1	12.101702000	-6.124075000	-0.782347000	1	11.583445000	2.479405000	-3.370152000
6	10.254461000	-6.253697000	3.473917000	1	14.325808000	0.213818000	-0.943074000
1	8.536784000	-6.039345000	4.763682000	6	12.595748000	-2.891602000	2.040619000
1	11.793453000	-6.387225000	1.967975000	1	10.886508000	-3.861368000	2.933833000
1	11.768697000	-5.769033000	-3.218297000	1	14.110478000	-1.759734000	1.001735000
1	10.926858000	-6.486345000	4.293836000	1	13.899390000	1.938631000	-2.679526000
6	-12.896672000	-0.190231000	1.217710000	1	13.310469000	-3.450563000	2.636645000
6	-12.937490000	0.093613000	-1.033665000	6	-11.356444000	-1.231540000	0.667228000
6	-12.529354000	-0.456258000	2.540610000	6	-11.473913000	0.359137000	-0.947257000
6	-14.237524000	0.114534000	0.866469000	6	-10.930191000	-2.177339000	1.605031000
6	-12.606748000	0.226993000	-2.385900000	6	-12.732956000	-1.037172000	0.381716000
6	-14.263103000	0.298030000	-0.569901000	6	-11.190502000	1.353385000	-1.888982000
6	-13.524403000	-0.394768000	3.514337000	6	-12.808034000	-0.020425000	-0.646898000
1	-11.507092000	-0.704594000	2.803055000	6	-11.906781000	-2.916859000	2.269428000
6	-15.218201000	0.170356000	1.864987000	1	-9.876925000	-2.334425000	1.808781000
6	-13.630028000	0.552050000	-3.274303000	6	-13.694137000	-1.793414000	1.064443000
1	-11.589758000	0.085964000	-2.734352000	6	-12.265771000	1.952621000	-2.542285000
6	-15.273060000	0.623242000	-1.484293000	1	-10.170642000	1.652062000	-2.104067000
6	-14.855505000	-0.081764000	3.185333000	6	-13.870514000	0.597495000	-1.318606000
1	-13.262980000	-0.595677000	4.549057000	6	-13.275695000	-2.727919000	2.007887000
1	-16.248281000	0.403187000	1.610642000	1	-11.600232000	-3.656169000	3.003458000
6	-14.951472000	0.745570000	-2.833388000	1	-14.751208000	-1.654592000	0.856448000
1	-13.397927000	0.659465000	-4.329735000	6	-13.593338000	1.579457000	-2.265937000
1	-16.292220000	0.781690000	-1.143463000	1	-12.070619000	2.726124000	-3.279145000
1	-15.605667000	-0.040471000	3.968973000	1	-14.896592000	0.316317000	-1.099264000
1	-15.725102000	0.996024000	-3.552632000	1	-14.010499000	-3.319717000	2.544904000
7	7.822151000	-5.372399000	0.214824000	1	-14.407608000	2.065294000	-2.794589000
7	-12.113420000	-0.201897000	0.058109000	7	9.998318000	-0.657154000	-0.320779000
6	3.021158000	3.533038000	-0.115232000	7	-10.598199000	-0.380361000	-0.144428000
6	3.486884000	4.142913000	-1.293216000				
6	3.338549000	4.144103000	1.110456000				
6	4.230378000	5.318689000	-1.252295000				
1	3.232734000	3.715718000	-2.257989000				
6	4.096613000	5.310137000	1.161400000				
1	3.021555000	3.682457000	2.040105000				
6	4.545090000	5.909588000	-0.022166000				
1	4.551732000	5.792692000	-2.173557000				
1	4.359464000	5.748002000	2.118414000				
6	4.935432000	8.294836000	0.659509000				

6	6.570957000	7.294270000	-0.556251000
6	3.755336000	8.602368000	1.343857000
6	5.963525000	9.256909000	0.483387000
6	7.367837000	6.389403000	-1.264566000
6	7.008129000	8.617738000	-0.289884000
6	3.626092000	9.887191000	1.867977000
1	2.964412000	7.870278000	1.461999000
6	5.808523000	10.541005000	1.020814000
6	8.606719000	6.835817000	-1.720742000
1	7.038215000	5.373632000	-1.451739000
6	8.257638000	9.041187000	-0.760199000
6	4.640860000	10.848590000	1.713935000
1	2.719255000	10.149005000	2.405016000
1	6.587650000	11.287156000	0.893852000
6	9.049666000	8.148090000	-1.476771000
1	9.242565000	6.151636000	-2.274733000
1	8.604664000	10.051624000	-0.563990000
1	4.508614000	11.839765000	2.136536000
1	10.019656000	8.463963000	-1.848064000
7	5.311302000	7.105125000	0.024522000

5. Electrochemical studies of monomers Cz_3N^* and Cz_2N^* .

CV experiments were performed in a three-electrode cell containing a GC or ITO electrode, Ag/AgCl reference electrode, and a Pt counter electrode in dichloromethane with TBAPF₆ as supporting electrolyte. The E_{HOMO} values were obtained from eq (S1) by incorporating the oxidation onset potential values obtained from CV, and LUMO levels were subsequently calculated using eq (S2) using optical band gaps obtained from the absorption edge calculated using eq (S3).

$$E_{HOMO} = - (4.8 - E_{1/2 Fc,Fc^+} + E_{Ox. Onset}) \quad \text{eq (S1)}$$

$$E_{g, \text{optical}} = (E_{LUMO} - E_{HOMO}) \quad \text{eq (S2)}$$

$$E_g \text{ (eV)} = 1240 / \lambda \text{ (nm)} \quad \text{eq (S3)}$$

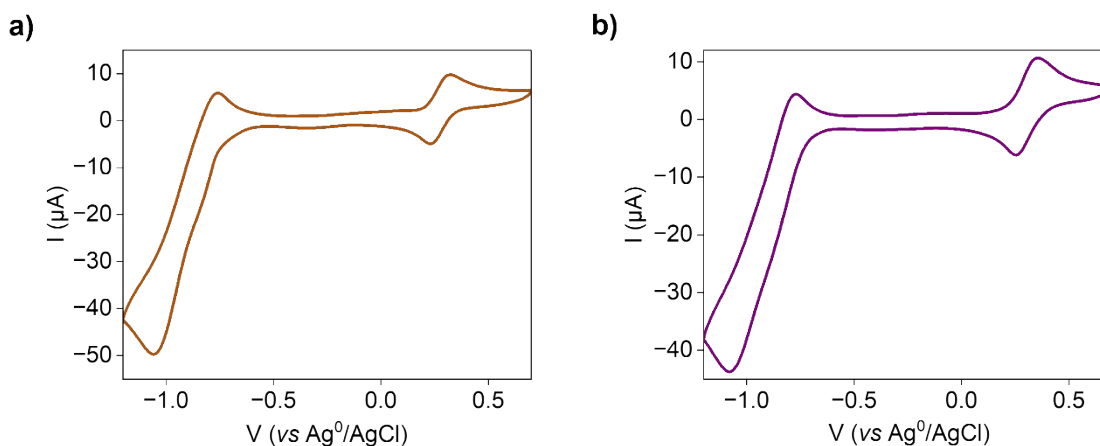


Fig. S4 CV curves of 1 mM a) Cz_3N^* , b) Cz_2N^* in CH_2Cl_2 with 0.2 M TBAPF₆ supporting electrolyte at a scan rate of 0.1 V s^{-1} .

6. Electropolymerisation studies of Cz_3N^+ and Cz_2N^+ :

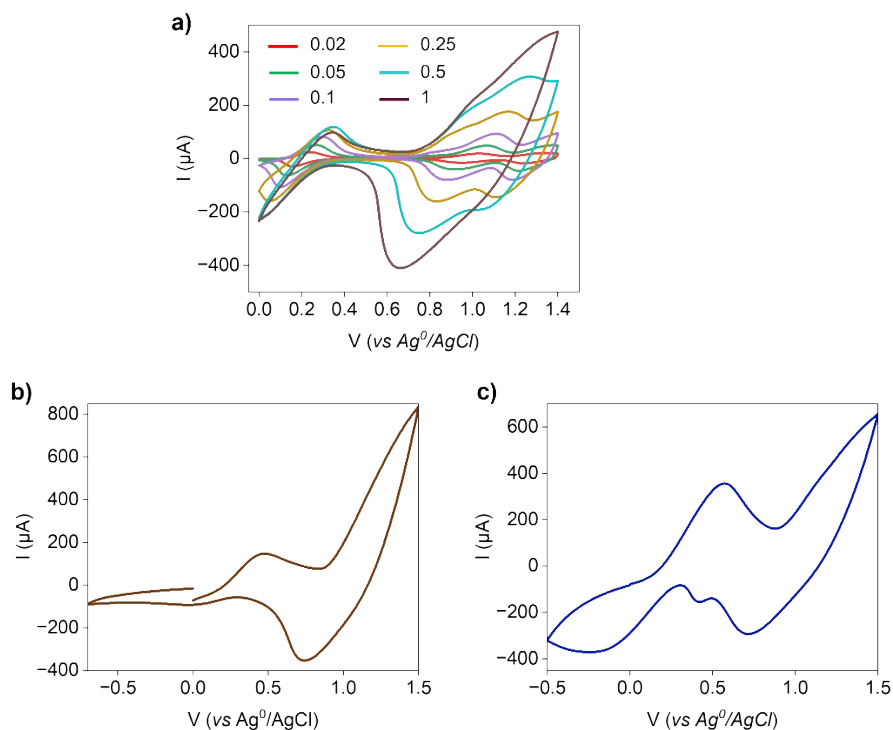


Fig. S5 a) CV of poly Cz_2N^+ , as-grown films on GC in monomer-free CH_2Cl_2 solutions with 0.1 M TBAPF₆ supporting electrolyte at different scan rate from 0.02 Vs⁻¹ to 1 V s⁻¹. b), c) CV of poly Cz_3N^+ , poly Cz_2N^+ as-grown polymer films on ITO electrode in monomer-free CH_2Cl_2 solutions with 0.1 M TBAPF₆ as supporting electrolyte at scan rate of 0.1 Vs⁻¹, respectively.

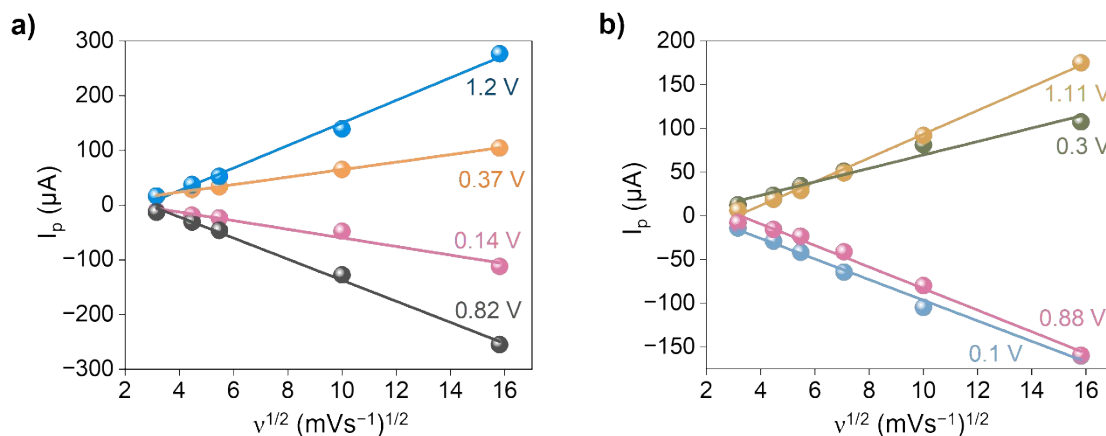
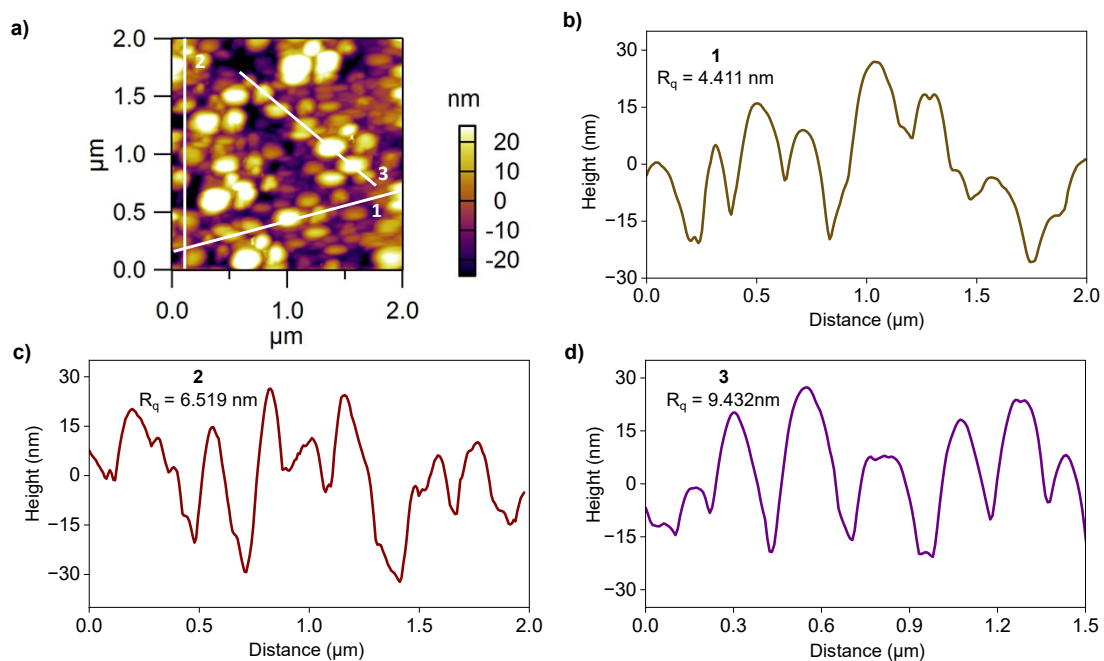


Fig. S6 Linear relationship of peak current vs square root of the scan rate for a) poly Cz_3N^+ and b) poly Cz_2N^+ on GC electrode.



7. AFM of polymeric thin film of polyCz₃N[•] and polyCz₂N[•].

Fig. S7 Cross-sectional line profiles. a) AFM image of polyCz₃N[•]@ITO film with a scan size of 2 μm. b) horizontal, c) vertical, and d) diagonal line profiles of the AFM image of the thin films were shown. The corresponding RMS roughness (R_q) values are shown in the inset.

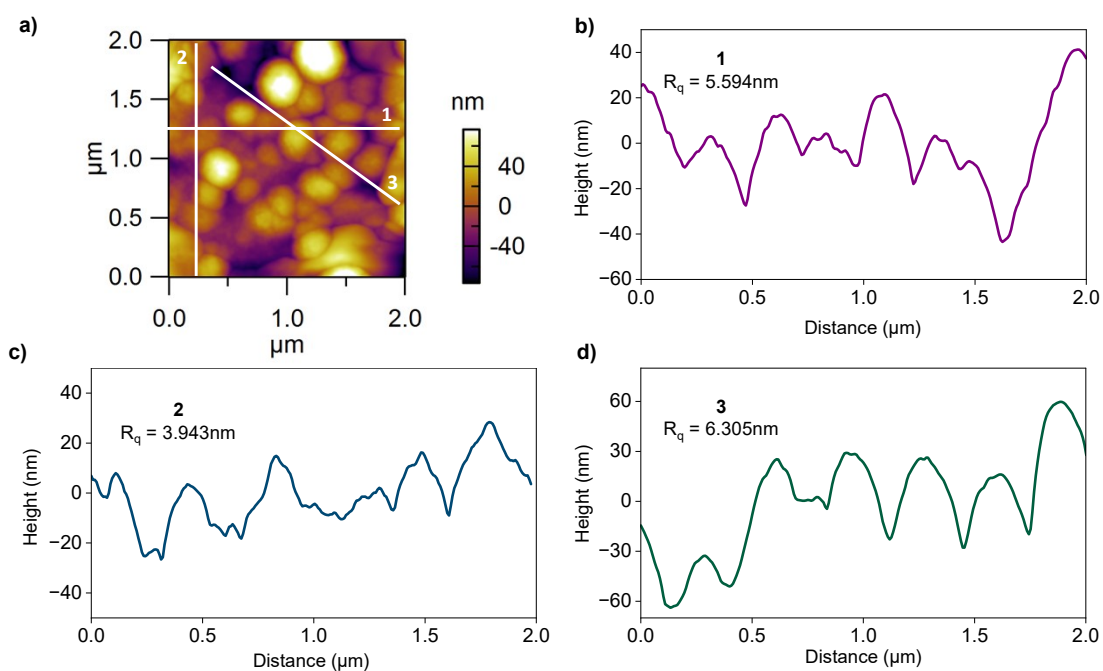


Fig. S8 Cross-sectional line profiles. a) AFM image of polyCz₂N@ITO film with a scan size of 2 μm. b) horizontal, c) vertical, and d) diagonal line profiles of the AFM image of the thin films were shown. The corresponding RMS roughness (R_q) values are shown in the inset.

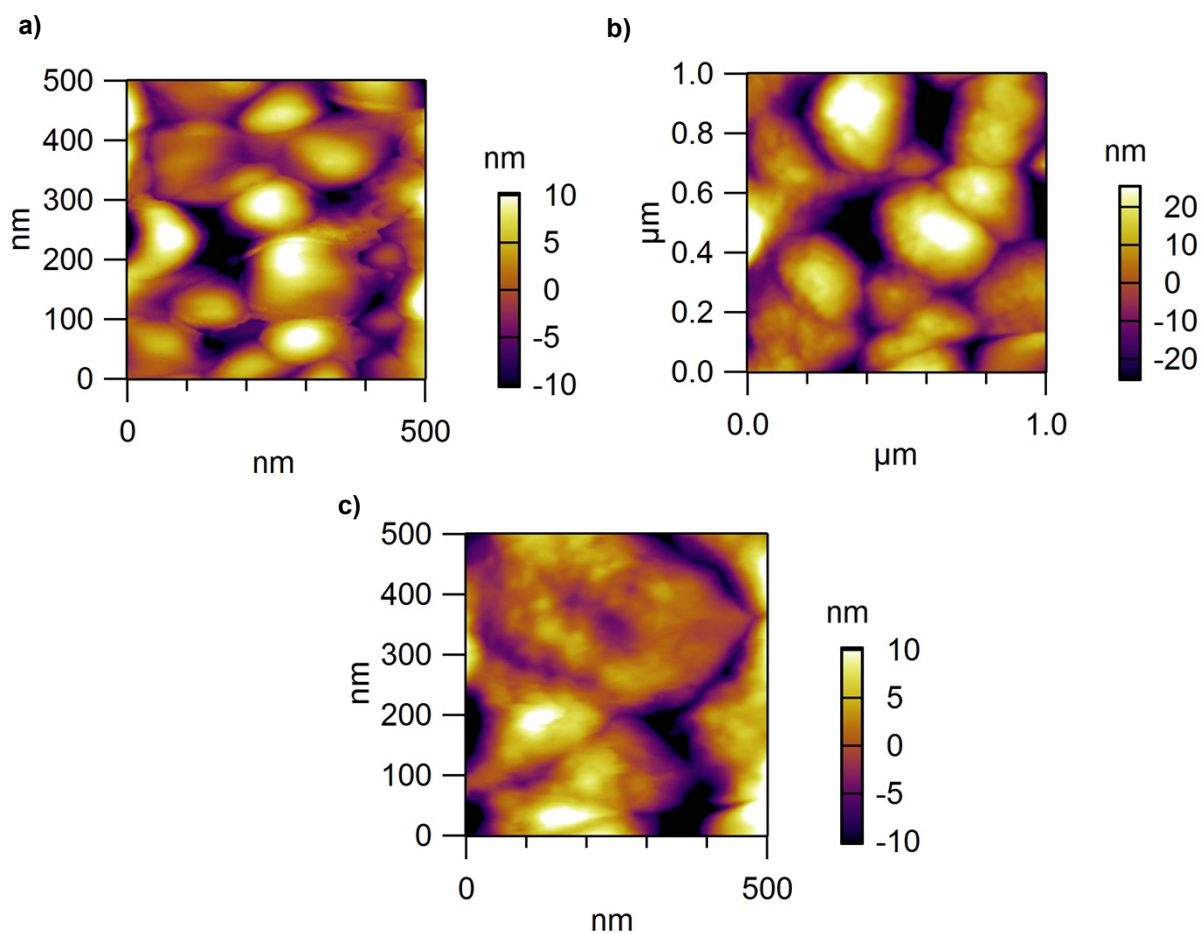


Fig. S9 Atomic force microscopy images of the Blatter radical films. 2D view of a) polyCz₃N[•]@ITO (scan size: 500 nm, RMS roughness: 0.698 ± 0.03 nm). b) polyCz₂N[•]@ITO (scan size: 1 μm, RMS roughness: 2.302 ± 0.122 nm). c) polyCz₂N[•]@ITO (scan size: 500 nm, RMS roughness: 0.809 ± 0.028 nm).

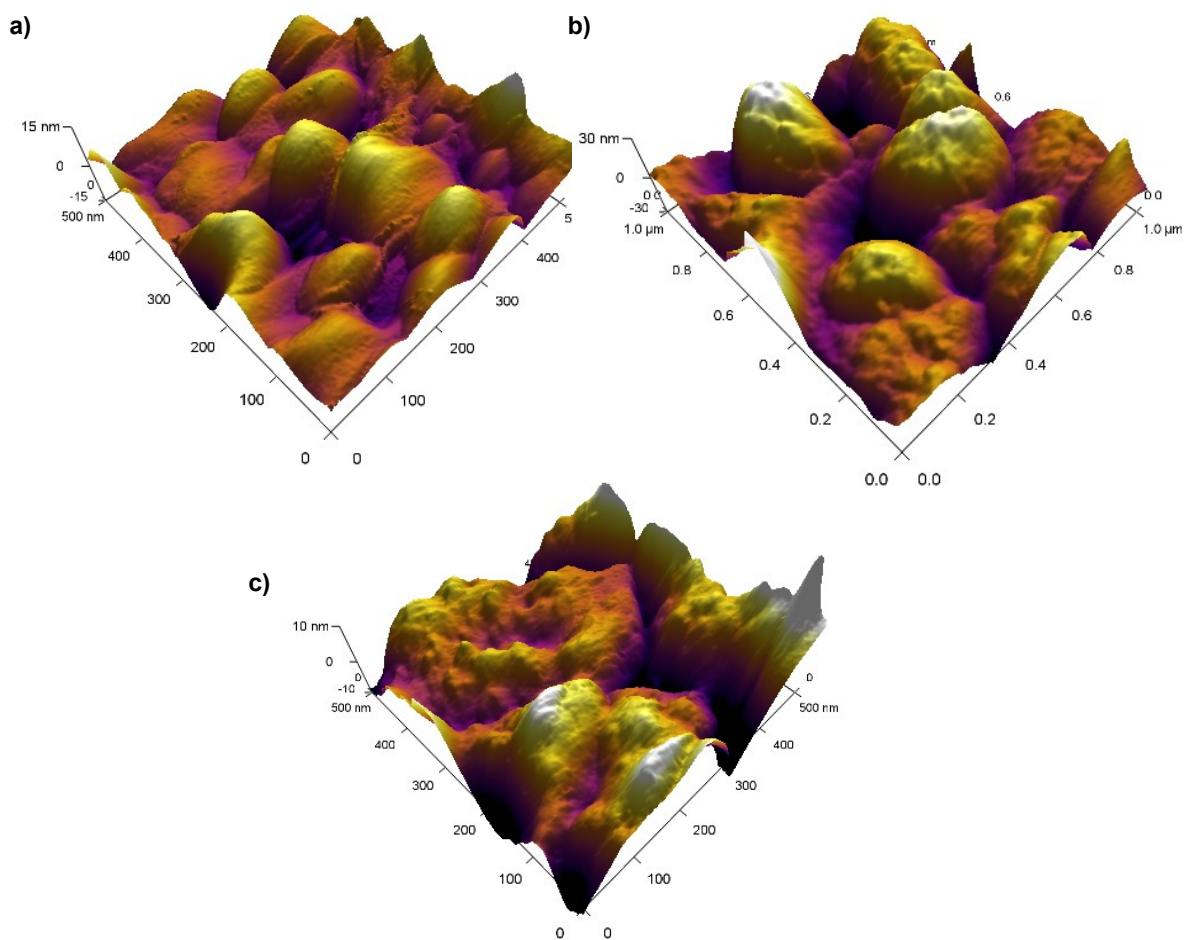


Fig. S10 Atomic force microscopy images of the Blatter radical films. 3D view of a) polyCz₃N•@ITO (scan size: 500 nm). b) polyCz₂N•@ITO (scan size: 1 μm). c) polyCz₂N•@ITO (scan size: 500 nm).

Table S5. RMS roughness values of thin film of poly Cz₃N* and polyCz₂N* for different scan size AFM images.

Thin film	Scan size	R _q (nm) Mean(μ)	R _q (nm) Standard Deviation(σ)	R _q (nm) Standard Error (SE)	Overall roughness(nm) ($\mu \pm SE$)
polyCz ₃ N*	2 $\mu\text{m} \times 2\mu\text{m}$	4.874	0.692	0.304	4.874 \pm 0.304
polyCz ₃ N*	0.5 $\mu\text{m} \times 0.5\mu\text{m}$	0.698	0.068	0.03	0.698 \pm 0.03
polyCz ₂ N*	2 $\mu\text{m} \times 2\mu\text{m}$	5.701	0.421	0.188	5.701 \pm 0.188
polyCz ₂ N*	1 $\mu\text{m} \times 1\mu\text{m}$	2.309	0.273	0.122	2.309 \pm 0.122
polyCz ₂ N*	0.5 $\mu\text{m} \times 0.5\mu\text{m}$	0.809	0.063	0.028	0.809 \pm 0.028

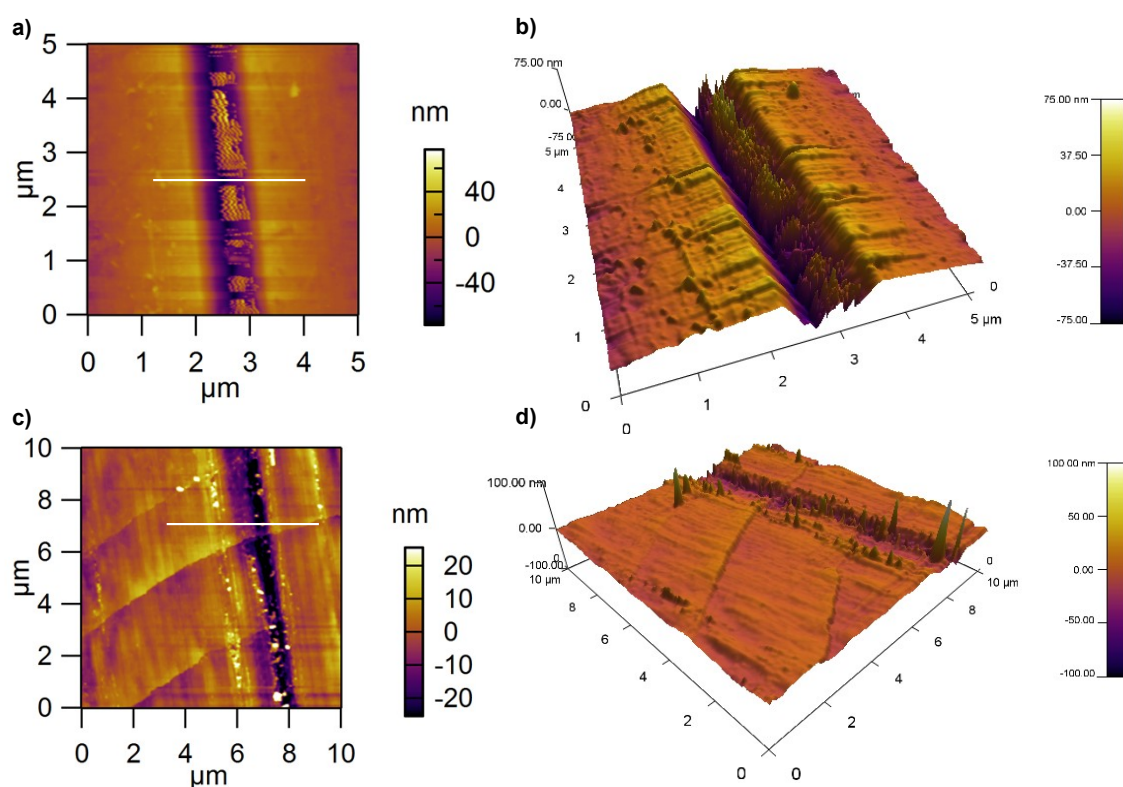


Fig. S11 Thickness measurements of and by scratching the films with a needle. a), b) 2D and 3D view of the polyCz₃N*@ITO film after scratching. c), d) 2D and 3D view of the polyCz₂N* @ITO film after scratching. The thickness was measured along the white line shown.

8. FTIR spectra of Cz_3N^+ , Cz_2N^+ , $\text{polyCz}_3\text{N}^+$ and $\text{polyCz}_2\text{N}^+$.

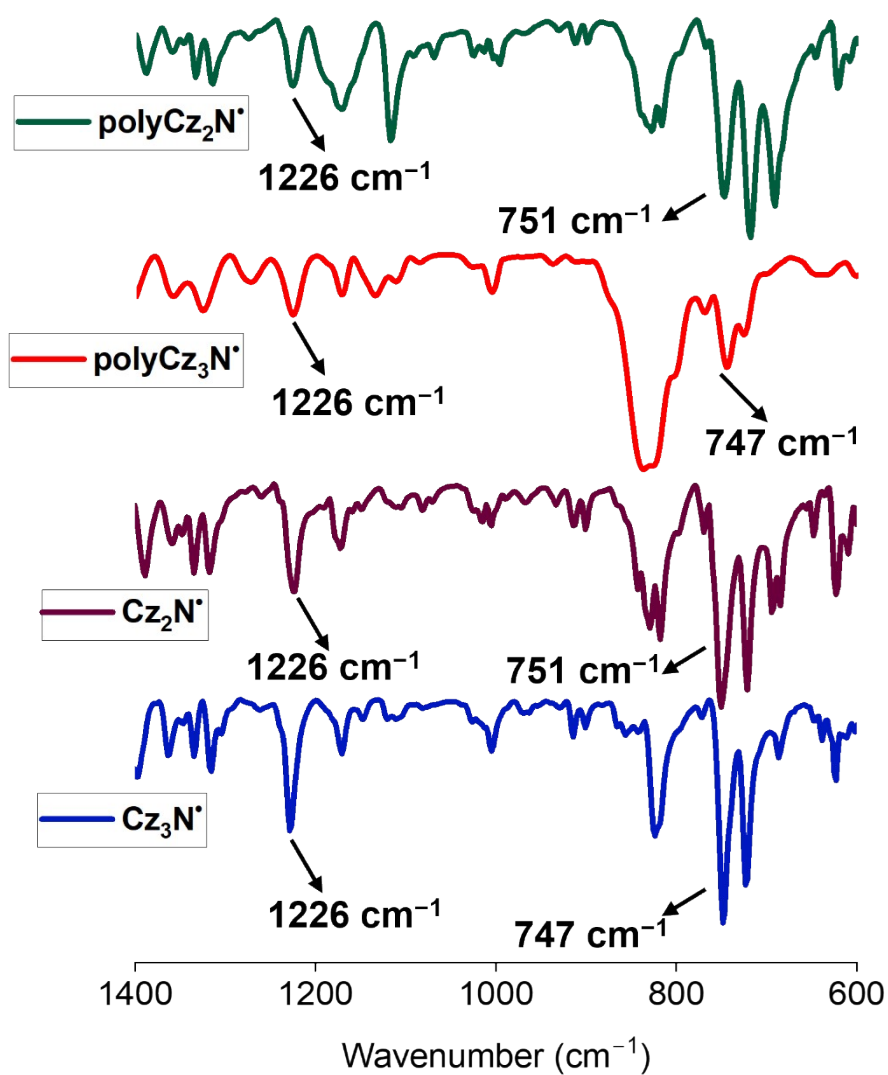
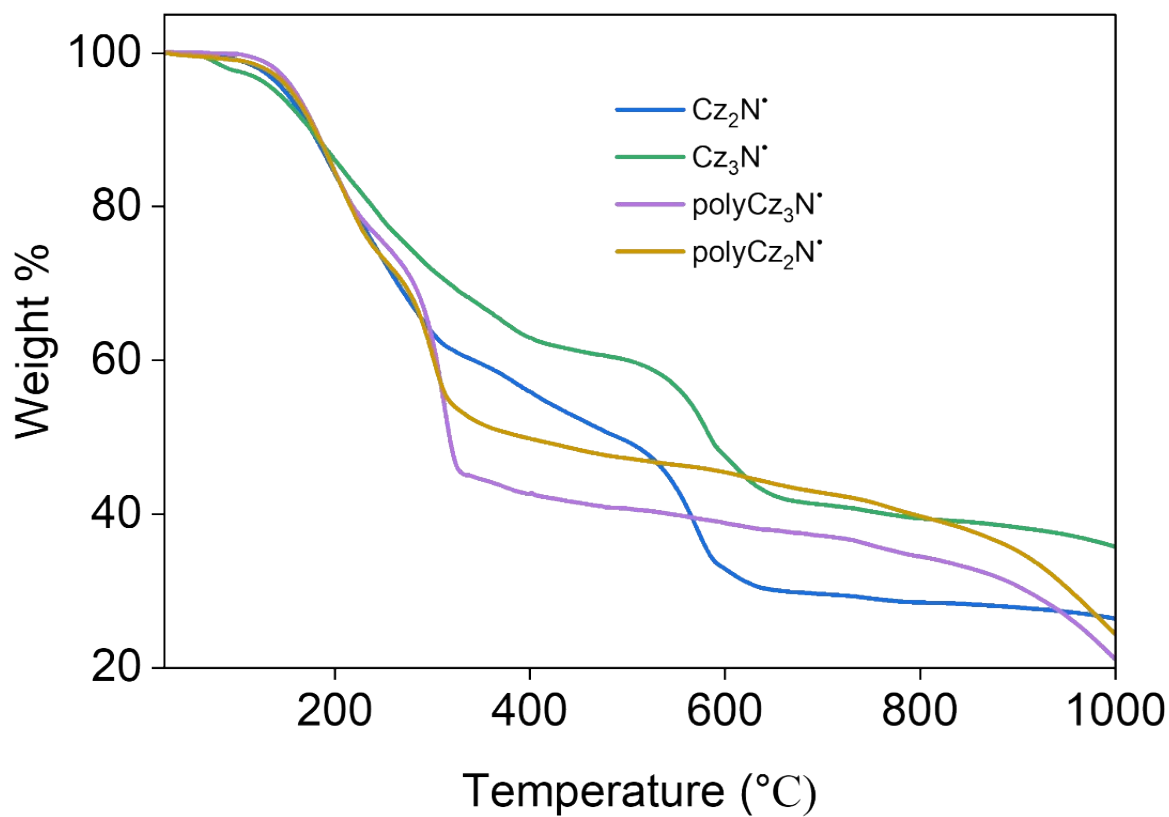


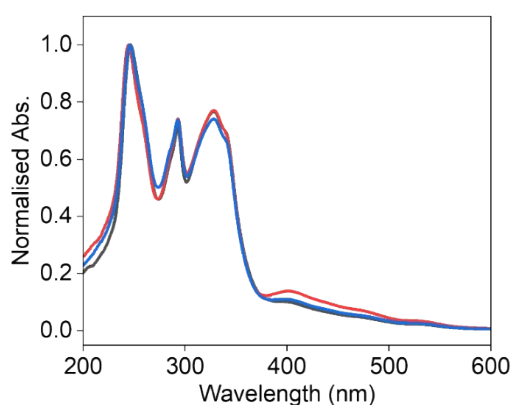
Fig. S12 FTIR spectra of polymer thin films compared to the spectra of the corresponding monomers, Cz_3N^+ (blue), Cz_2N^+ (wine), $\text{polyCz}_3\text{N}^+$ (red) and $\text{polyCz}_2\text{N}^+$ (green).



9. Thermogravimetric analysis (TGA) of Cz₃N*, Cz₂N*, polyCz₃N* and polyCz₂N*.

Fig. S13 TGA of Cz₃N* (green), Cz₂N* (blue), polyCz₃N* (purple) and polyCz₂N* (yellow) under N₂ atmosphere in the temperature range of 25 – 1000 °C at a heating rate of 10 °C/min.

10. Air-stability of Cz_3N^{\bullet} radical examined by solution state UV-Vis absorption



spectroscopy.

Fig. S14 UV-Vis absorption spectra of Cz_3N^{\bullet} in tetrahydrofuran on day 1 (red), day 10 (blue), and day 20 (black).

11. XPS studies of monomers Cz_3N^{\bullet} and Cz_2N^{\bullet} and polymers $polyCz_3N^{\bullet}$ and $polyCz_2N^{\bullet}$.

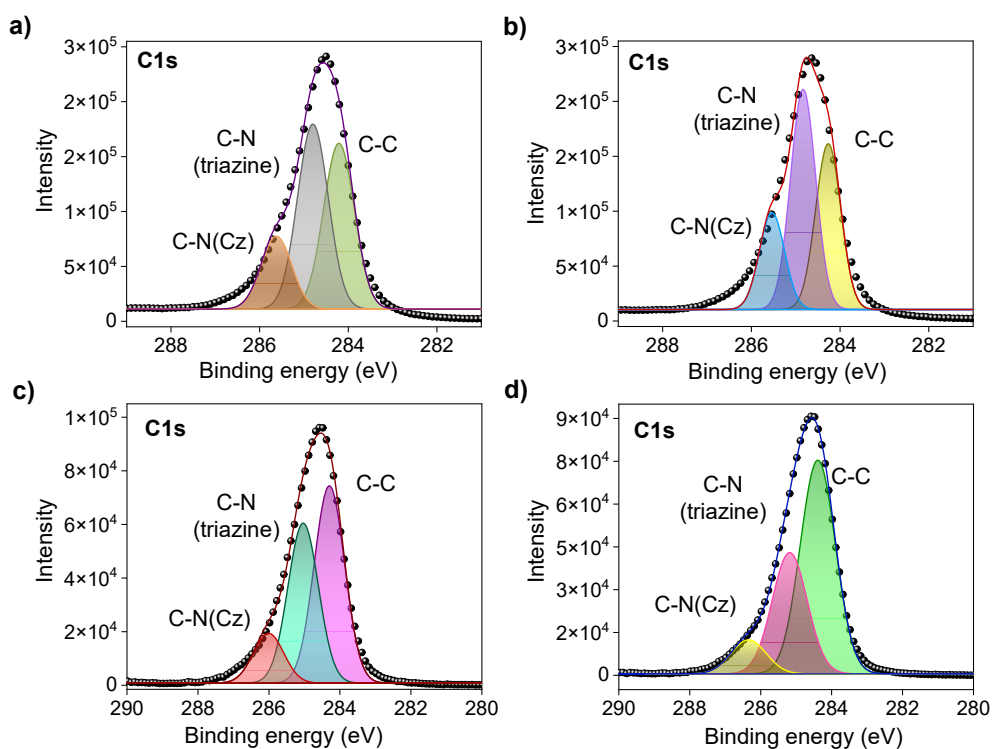


Fig. S15 Fitted C1s XPS spectra of a) Cz_3N^\bullet b) Cz_2N^\bullet c) $polyCz_3N^\bullet$ and d) $polyCz_2N^\bullet$, respectively.

12. Concentration-dependent absorption spectra of radical monomers.

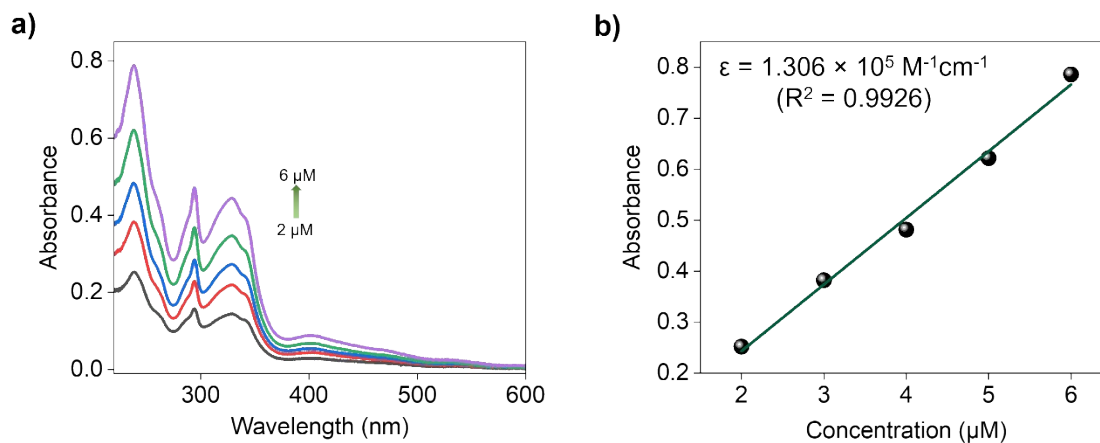


Fig. S16 a) Concentration-dependent absorption spectra of Cz_3N^\bullet in CH_2Cl_2 and b) molar extinction coefficient calculated at $\lambda_{max} = 238$ nm.

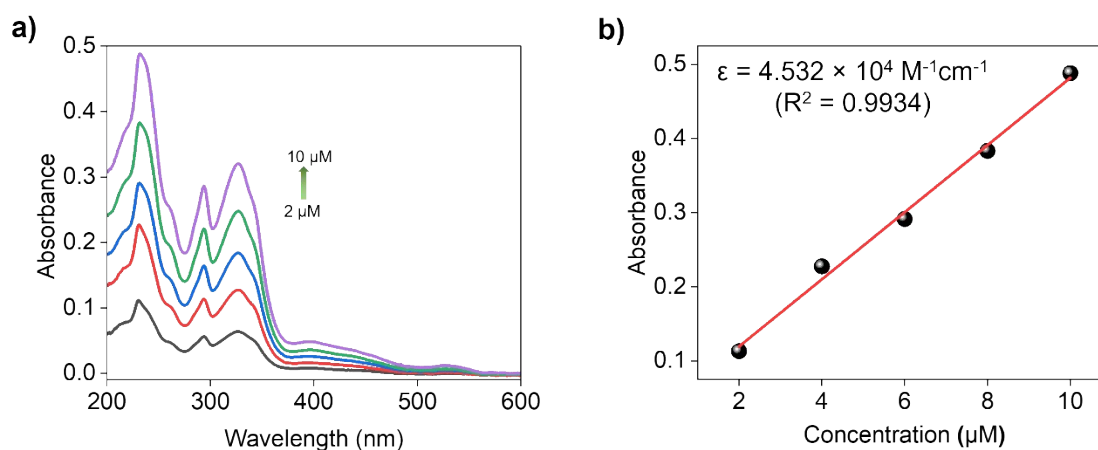
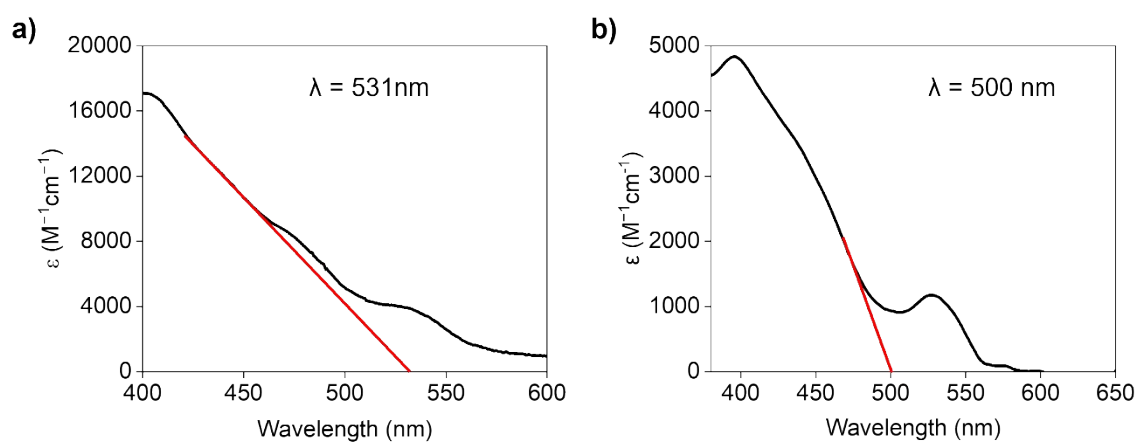


Fig. S17 a) Concentration-dependent absorption spectra of Cz_2N^\bullet in CH_2Cl_2 and b) molar extinction coefficient calculated at $\lambda_{max} = 232$ nm.

13. Band gap calculation for monomer radicals, Cz_3N^\bullet , Cz_2N^\bullet and oxidised species Cz_3N^+ , Cz_2N^+ and for polymeric thin film $polyCz_3N^\bullet$ and $polyCz_2N^\bullet$.



Cz_2N^+ and for polymeric thin film $polyCz_3N^\bullet$ and $polyCz_2N^\bullet$.

Fig. S18 Absorption onset wavelengths of a) Cz_3N^\bullet and b) Cz_2N^\bullet obtained from the absorption spectra in CH_2Cl_2 . Band gaps were calculated using eq. S3 and the corresponding E_g values are 2.33 and 2.48 eV for Cz_3N^\bullet and Cz_2N^\bullet , respectively.

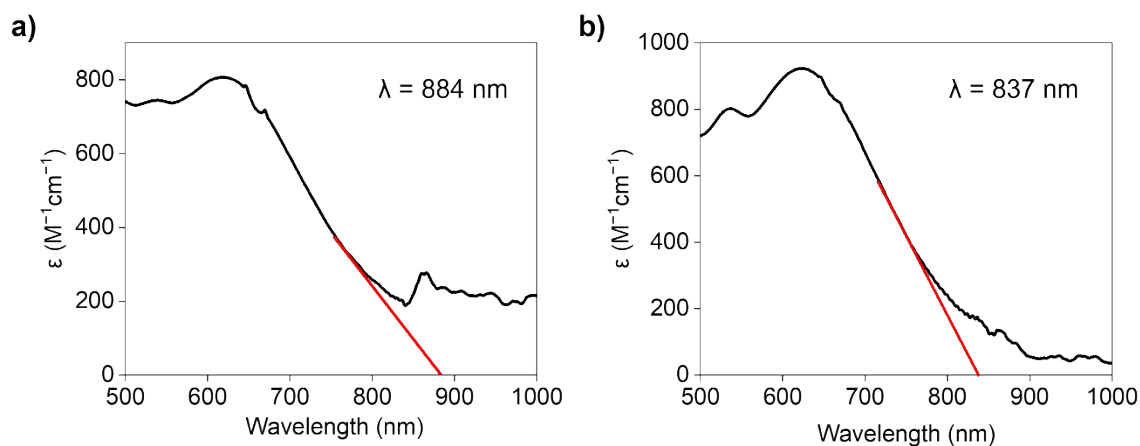


Fig. S19 Absorption onset wavelengths of a) Cz_3N^+ and b) Cz_2N^+ obtained from the absorption spectra in CH_2Cl_2 . Band gaps were calculated using eq. S3 and the corresponding E_g values are 1.40 and 1.48 eV for Cz_3N^+ and Cz_2N^+ , respectively.

14. DFT-optimized geometries of Cz_3N^+ and Cz_2N^+ using DCM as solvent.

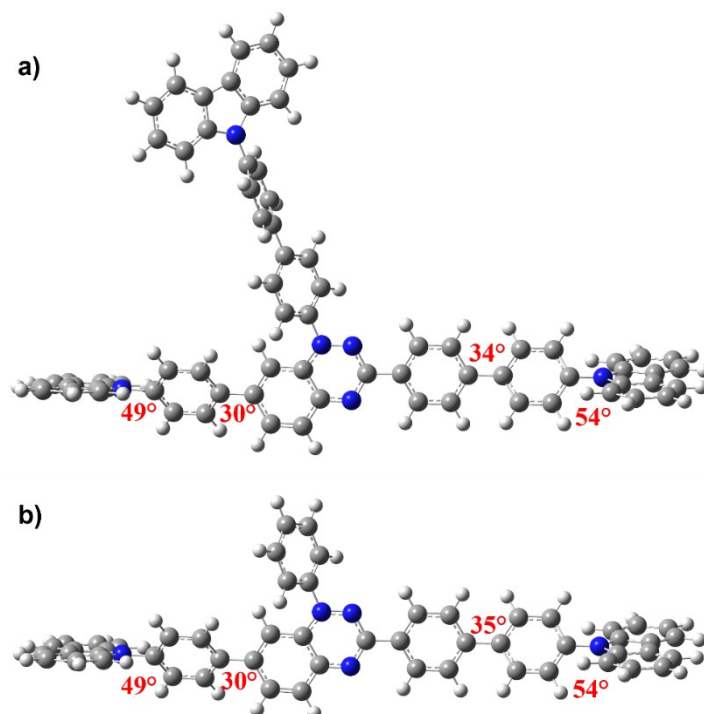


Fig. S20 DFT-optimized geometries of a) Cz_3N^+ and b) Cz_2N^+ . The torsional angles are shown in red colour.

Table S6. Cartesian coordinates.

Cz_3N^+				Cz_2N^+			
6	1.303170000	-5.182271000	-0.576284000	6	3.604522000	-1.426924000	-1.593244000
6	-0.037151000	-4.939084000	-0.672429000	6	2.243560000	-1.456418000	-1.697575000
6	-0.530665000	-3.609068000	-0.543638000	6	1.450598000	-0.570587000	-0.912681000
6	0.428564000	-2.545617000	-0.369857000	6	2.132796000	0.371075000	-0.057328000
6	1.800498000	-2.821661000	-0.234264000	6	3.534387000	0.366243000	0.056149000
6	2.255913000	-4.130182000	-0.336755000	6	4.285089000	-0.522304000	-0.703206000
1	1.664373000	-6.197295000	-0.693050000	1	4.194872000	-2.095260000	-2.209023000
1	-0.756190000	-5.732782000	-0.836845000	1	1.731335000	-2.143421000	-2.360570000
1	2.489530000	-2.019479000	-0.011353000	1	4.016791000	1.027453000	0.761947000
6	-2.247756000	-2.104280000	-0.390528000	6	-0.572923000	0.196624000	-0.166442000
6	3.688267000	-4.447977000	-0.204450000	6	5.754742000	-0.548465000	-0.610528000
6	4.677169000	-3.522847000	-0.592335000	6	6.484657000	0.617764000	-0.308653000
6	4.110757000	-5.684683000	0.320682000	6	6.472799000	-1.742884000	-0.814611000
6	6.027402000	-3.814853000	-0.456425000	6	7.868742000	0.593423000	-0.208022000
1	4.392065000	-2.569006000	-1.023094000	1	5.968689000	1.561614000	-0.169407000
6	5.459899000	-5.984166000	0.457275000	6	7.857626000	-1.774083000	-0.716796000
1	3.381551000	-6.418938000	0.645394000	1	5.947757000	-2.666127000	-1.034256000
6	6.433945000	-5.051099000	0.070247000	6	8.571478000	-0.604867000	-0.411721000

1	6.771509000	-3.082232000	-0.746788000	1	8.409287000	1.499396000	0.040270000
1	5.762718000	-6.948185000	0.849208000	1	8.391447000	-2.700778000	-0.892434000
6	-3.687284000	-1.809387000	-0.329052000	6	-2.041231000	0.121261000	-0.150075000
6	-4.620895000	-2.854335000	-0.432823000	6	-2.702727000	-0.819319000	-0.957716000
6	-4.155467000	-0.494373000	-0.161621000	6	-2.805970000	0.976813000	0.662373000
6	-5.982236000	-2.589237000	-0.369972000	6	-4.088700000	-0.898591000	-0.952435000
1	-4.269613000	-3.872272000	-0.553178000	1	-2.121690000	-1.489162000	-1.580369000
6	-5.518265000	-0.237344000	-0.099784000	6	-4.191540000	0.891042000	0.662261000
1	-3.449121000	0.324280000	-0.091577000	1	-2.311841000	1.714741000	1.283124000
6	-6.462506000	-1.276600000	-0.201809000	6	-4.864610000	-0.046106000	-0.144361000
1	-6.683189000	-3.415365000	-0.426612000	1	-4.576523000	-1.648888000	-1.565599000
1	-5.856649000	0.788205000	0.003358000	1	-4.762052000	1.579349000	1.276743000
7	-0.112523000	-1.283818000	-0.314764000	7	1.308228000	1.218063000	0.639493000
7	-1.408527000	-1.051342000	-0.298199000	7	-0.004335000	1.137059000	0.617789000
7	-1.840999000	-3.371988000	-0.563766000	7	0.122049000	-0.632982000	-0.961652000
6	0.700054000	-0.089378000	-0.257379000	6	1.819431000	2.282264000	1.483567000
6	0.435295000	0.849460000	0.741770000	6	1.404600000	2.325448000	2.815149000
6	1.682663000	0.136664000	-1.224812000	6	2.659094000	3.253388000	0.934334000
6	1.187222000	2.016163000	0.784998000	6	1.867115000	3.361876000	3.622945000
1	-0.344229000	0.662093000	1.470857000	1	0.744775000	1.558810000	3.204244000
6	2.419171000	1.314203000	-1.170860000	6	3.104276000	4.288110000	1.755593000
1	1.858116000	-0.581927000	-2.017589000	1	2.934241000	3.217533000	-0.113791000
6	2.193999000	2.273382000	-0.165530000	6	2.714800000	4.339900000	3.096131000
1	0.973478000	2.748346000	1.555542000	1	1.564238000	3.403548000	4.663549000
1	3.190476000	1.481322000	-1.914192000	1	3.747423000	5.057373000	1.342272000
6	-7.916405000	-0.997421000	-0.134074000	1	3.068169000	5.146504000	3.729850000
6	-8.833687000	-1.743097000	-0.895177000	6	-6.344076000	-0.131223000	-0.144777000
6	-8.421344000	0.021127000	0.693211000	6	-7.051003000	-0.436721000	-1.321054000
6	-10.200112000	-1.489425000	-0.828842000	6	-7.083832000	0.092381000	1.029720000
1	-8.475996000	-2.524272000	-1.557840000	6	-8.439713000	-0.522363000	-1.325608000
6	-9.784886000	0.291180000	0.753801000	1	-6.511561000	-0.596971000	-2.248870000
1	-7.742960000	0.603635000	1.307937000	6	-8.473494000	0.022649000	1.030324000
6	-10.686562000	-0.465985000	-0.005238000	1	-6.568245000	0.312244000	1.958902000
1	-10.893557000	-2.085588000	-1.411868000	6	-9.162818000	-0.288899000	-0.148779000
1	-10.153943000	1.091340000	1.386104000	1	-8.966887000	-0.773487000	-2.239541000
6	8.784312000	-5.203193000	-0.792515000	1	-9.028012000	0.213304000	1.942694000
6	8.428381000	-5.857082000	1.360437000	6	10.866083000	0.258310000	-0.943615000
6	8.646985000	-4.786469000	-2.119804000	6	10.735061000	-1.558764000	0.424474000
6	10.036553000	-5.615217000	-0.272087000	6	10.597713000	1.314184000	-1.819607000
6	7.885858000	-6.124314000	2.620779000	6	12.194205000	-0.103048000	-0.605707000
6	9.810926000	-6.026942000	1.098803000	6	10.306464000	-2.600296000	1.252503000
6	9.793043000	-4.760140000	-2.913262000	6	12.110672000	-1.255805000	0.268351000
1	7.685284000	-4.499308000	-2.528806000	6	11.682804000	2.024628000	-2.331055000
6	11.172659000	-5.579849000	-1.089067000	1	9.584664000	1.574240000	-2.103624000
6	8.747217000	-6.593978000	3.611319000	6	13.266809000	0.625549000	-1.132848000
1	6.834444000	-5.967963000	2.832168000	6	11.281756000	-3.356124000	1.901513000
6	10.655274000	-6.499670000	2.110260000	1	9.254137000	-2.815621000	1.396755000
6	11.045422000	-5.146271000	-2.406176000	6	13.070808000	-2.028999000	0.931432000
1	9.710960000	-4.436969000	-3.946551000	6	13.004524000	1.691188000	-1.989896000
1	12.137688000	-5.892527000	-0.701334000	1	11.497971000	2.850837000	-3.010824000
6	10.116690000	-6.786447000	3.361895000	1	14.288730000	0.357693000	-0.881364000
1	8.347255000	-6.811515000	4.597002000	6	12.650397000	-3.080740000	1.741412000
1	11.716180000	-6.634358000	1.921475000	1	10.972336000	-4.172616000	2.546825000
1	11.918351000	-5.112201000	-3.050358000	1	14.127829000	-1.806384000	0.819607000
1	10.759404000	-7.155524000	4.154886000	1	13.826651000	2.265824000	-2.404657000
6	-12.850853000	-0.149760000	1.227723000	1	13.384072000	-3.689969000	2.259767000

6	-12.915778000	0.062882000	-1.033201000	6	-11.359712000	-1.157296000	0.702635000
6	-12.471941000	-0.378595000	2.554145000	6	-11.438077000	0.337045000	-1.006651000
6	-14.194482000	0.144650000	0.880350000	6	-10.957974000	-2.054937000	1.696676000
6	-12.600515000	0.157108000	-2.392274000	6	-12.729592000	-0.959794000	0.390979000
6	-14.235309000	0.283071000	-0.560874000	6	-11.132529000	1.271895000	-2.000615000
6	-13.457994000	-0.287492000	3.534910000	6	-12.779674000	-0.004659000	-0.696755000
1	-11.448417000	-0.622436000	2.815513000	6	-11.952890000	-2.740243000	2.391668000
6	-15.165977000	0.231082000	1.885429000	1	-9.909777000	-2.218657000	1.920059000
6	-13.633996000	0.456284000	-3.278209000	6	-13.709595000	-1.660691000	1.104932000
1	-11.587887000	0.007266000	-2.749378000	6	-12.193611000	1.847880000	-2.696914000
6	-15.255766000	0.581681000	-1.472415000	1	-10.107309000	1.545402000	-2.223163000
6	-14.791387000	0.017839000	3.209292000	6	-13.827580000	0.588359000	-1.412047000
1	-13.187203000	-0.459125000	4.572428000	6	-13.315685000	-2.545487000	2.105145000
1	-16.198171000	0.456747000	1.633570000	1	-11.665367000	-3.441357000	3.169487000
6	-14.950016000	0.663202000	-2.828233000	1	-14.761997000	-1.518313000	0.877025000
1	-13.413758000	0.532660000	-4.338820000	6	-13.528438000	1.509888000	-2.411926000
1	-16.270551000	0.751478000	-1.124366000	1	-11.980910000	2.575232000	-3.474709000
1	-15.534260000	0.083076000	3.998143000	1	-14.859266000	0.335236000	-1.185427000
1	-15.731858000	0.892620000	-3.545520000	1	-14.065194000	-3.094126000	2.666976000
7	7.806302000	-5.352850000	0.205514000	1	-14.331175000	1.975944000	-2.974796000
7	-12.079102000	-0.198681000	0.059599000	7	9.979207000	-0.632175000	-0.314186000
6	2.991277000	3.520011000	-0.109536000	7	-10.580187000	-0.366599000	-0.151411000
6	3.436240000	4.151037000	-1.284774000				
6	3.326553000	4.107916000	1.123042000				
6	4.176521000	5.327168000	-1.233697000				
1	3.164893000	3.745136000	-2.253880000				
6	4.084813000	5.272034000	1.182849000				
1	3.029348000	3.628015000	2.049790000				
6	4.512642000	5.895578000	0.002714000				
1	4.477147000	5.820362000	-2.151404000				
1	4.366297000	5.688575000	2.143611000				
6	4.939105000	8.246707000	0.771580000				
6	6.502215000	7.307739000	-0.586433000				
6	3.799634000	8.522770000	1.533410000				
6	5.955215000	9.217359000	0.579432000				
6	7.260759000	6.438993000	-1.376939000				
6	6.952726000	8.617978000	-0.283264000				
6	3.702705000	9.782536000	2.122011000				
1	3.012694000	7.788362000	1.661887000				
6	5.833818000	10.475539000	1.182093000				
6	8.471518000	6.911048000	-1.880978000				
1	6.926431000	5.430086000	-1.590174000				
6	8.172817000	9.068180000	-0.802567000				
6	4.708609000	10.750305000	1.954690000				
1	2.827871000	10.018869000	2.720298000				
1	6.605145000	11.227551000	1.043626000				
6	8.924678000	8.212555000	-1.603263000				
1	9.076624000	6.254963000	-2.499486000				
1	8.528916000	10.069556000	-0.578762000				
1	4.602701000	11.721048000	2.428790000				
1	9.871503000	8.549417000	-2.013608000				
7	5.277004000	7.087311000	0.058903000				

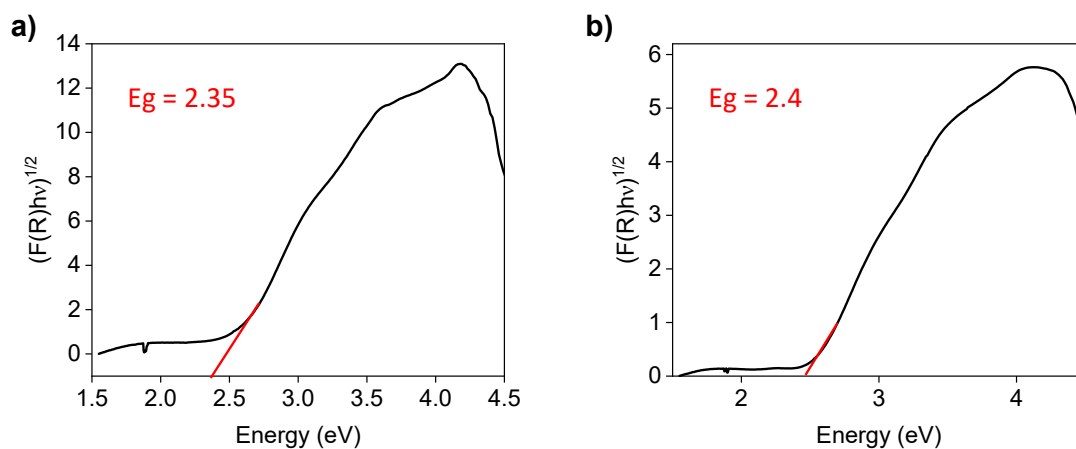


Fig. S21 Band gap calculated by using Tauc's method of a) polyCz₃N* and b) polyCz₂N* coated on an ITO substrate.

The band gap for the polymer thin films was calculated from a Tauc plot of $(\alpha hv)^{1/2}$ vs. energy (eV), where $F(R)$ or α is the absorption coefficient, obtained from the reflectance spectra of the polymer films. The reflectance spectra were directly measured on the UV/vis spectrometer by choosing the reflectance spectra mode in the instrument parameters.

15. Experimentally calculated HOMO-LUMO and band gap for Cz_3N^+ , Cz_2N^+ , $\text{polyCz}_3\text{N}^+$, and $\text{polyCz}_2\text{N}^+$.

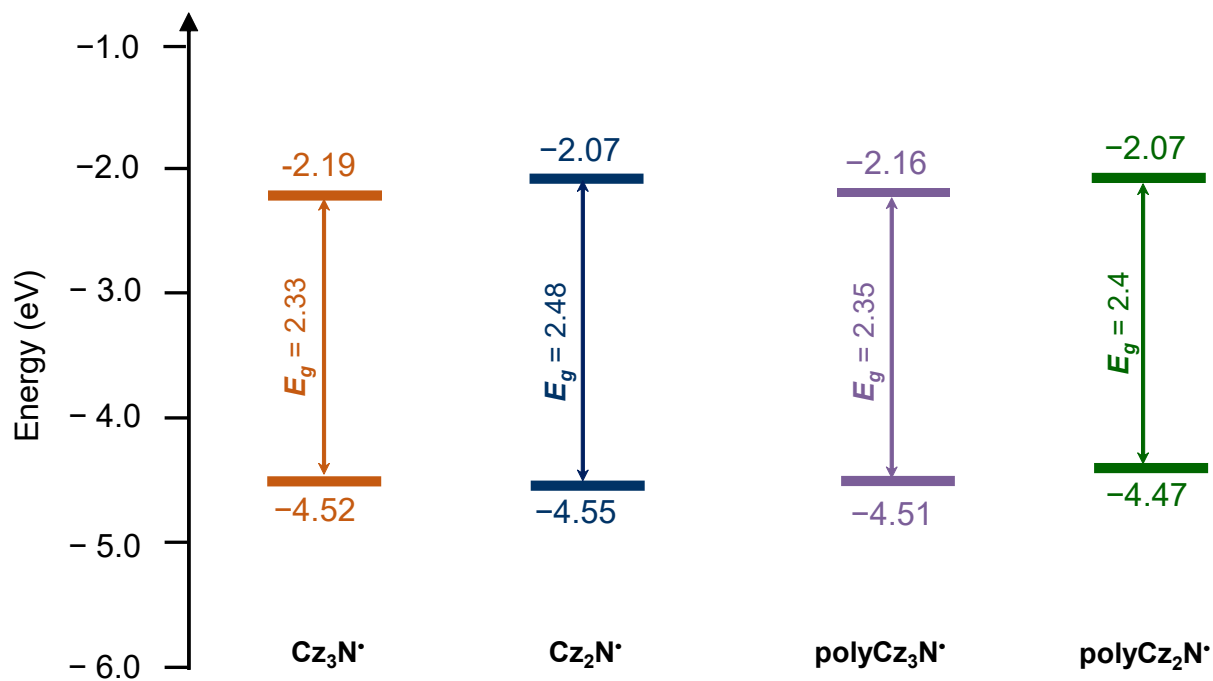


Fig. S22 HOMO-LUMO energy level diagram representing the experimental band gaps of Cz_3N^+ , Cz_2N^+ , $\text{polyCz}_3\text{N}^+$, and $\text{polyCz}_2\text{N}^+$.

Table S7. Comparison of theoretical and experimental energy values with NHE

	Theoretical (vs Vacuum)		V vs NHE*	
	HOMO (eV)	LUMO (eV)	HOMO or VB	LUMO or CB
Cz ₃ N•	-5.66	-3.00	1.22	-1.44
Cz ₂ N•	-5.67	-2.97	1.23	-1.47
Cz ₃ N ⁺	-5.86	-4.53	1.42	0.09
Cz ₃ N ⁺	-5.86	-4.53	1.36	0.09
	Experimental (vs Ag/AgCl)		eV (vs NHE)#	
	HOMO	LUMO	HOMO	LUMO
Cz ₃ N•	-4.52	-2.19	-4.23	-1.9
Cz ₂ N•	-4.55	-2.07	-4.26	-1.78
polyCz ₃ N•	-4.51	-2.16	-4.22	-1.87
polyCz ₂ N•	-4.47	-2.07	-4.18	-1.78

$$*E_{NHE} = -(-E_{vacuum} + 4.44) \text{ V}$$

$$\#E_{NHE} = (E_{Ag/AgCl} + 0.288) \text{ V}$$

16. EPR studies of Cz₃N• and Cz₂N•.

Table S8. Experimental hyperfine coupling constants (G) for different Blatter radicals in toluene.

S. No.	Cz _x N•	<i>a</i> _{hfc} (G)		
		N1	N2	N _{rad}

1	Cz ₃ N*	7.31	4.84	4.84
2	Cz ₂ N*	7.4	4.91	4.82

17. References:

1. M. J. Frisch, G. W. Trucks, H. B. Schlegel, G. E. Scuseria, M. A. Robb, J. R. Cheeseman, G. Scalmani, V. Barone, G. A. Petersson, H. Nakatsuji, X. Li, M. Caricato, A. V. Marenich, J. Bloino, B. G. Janesko, R. Gomperts, B. Mennucci, H. P. Hratchian, J. V. Ortiz, A. F. Izmaylov, J. L. Sonnenberg, D. Williams-Young, F. Ding, F. Lipparini, F. Egidi, J. Goings, B. Peng, A. Petrone, T. Henderson, D. Ranasinghe, V. G. Zakrzewski, J. Gao, N. Rega, G. Zheng, W. Liang, M. Hada, M. Ehara, K. Toyota, R. Fukuda, J. Hasegawa, M. Ishida, T. Nakajima, Y. Honda, O. Kitao, H. Nakai, T. Vreven, K. Throssell, J. A. Montgomery Jr., J. E. Peralta, F. Ogliaro, M. J. Bearpark, J. J. Heyd, E. N. Brothers, K. N. Kudin, V. N. Staroverov, T. A. Keith, R. Kobayashi, J. Normand, K. Raghavachari, A. P. Rendell, J. C. Burant, S. S. Iyengar, J. Tomasi, M. Cossi, J. M. Millam, M. Klene, C. Adamo, R. Cammi, J. W. Ochterski, R. L. Martin, K. Morokuma, O. Farkas, J. B. Foresman, D. J. Fox, Gaussian 16 Rev. C.01, 2016.
2. S. Stoll, A. Schweiger, *J. Magn. Reson.*, 2006, **178**, 42-55.
3. SAINT+ Software for CCD Diffractometers; Bruker AXS: Madison, WI, 2000.
4. G. M. Sheldrick, SADABS 2.0; University of Göttingen: Göttingen, Germany, 2000.
5. G. M. Sheldrick, SHELXL-2014: Program for Crystal Structure Refinement; University of Göttingen: Göttingen, Germany, 2014.
6. O. V. Dolomanov, L. J. Bourhis, R. J. Gildea, J. A. Howard, H. Puschmann, *J. Appl. Crystallogr.*, 2009, **42**, 339–341.
7. M. E. Filkina, D. N. Baray, E. K. Beloglazkina, Y. K. Grishin, V. A. Roznyatovsky, M. E. Kukushkin, *Int. J. Mol. Sci.*, 2023, **24**, 1289.
8. R. Liu, Z. Li, S. Liu, J. Zheng, P. Zhu, B. Cheng, R. Yu, H. Geng, *J. Agric. Food Chem.*, 2023, **71**, 6803–6817.
9. A. A. Berezin, G. Zissimou, C. P. Constantinides, Y. Beldjoudi, J. M. Rawson, P. A. Koutentis, *J. Org. Chem.*, 2014, **79**, 314–327.
10. P. Bartos, P. Szamweber, B. Camargo, A. Pietrzak, P. Kaszyński, *Chem. Sci.*, 2025, **16**, 12139-12147.